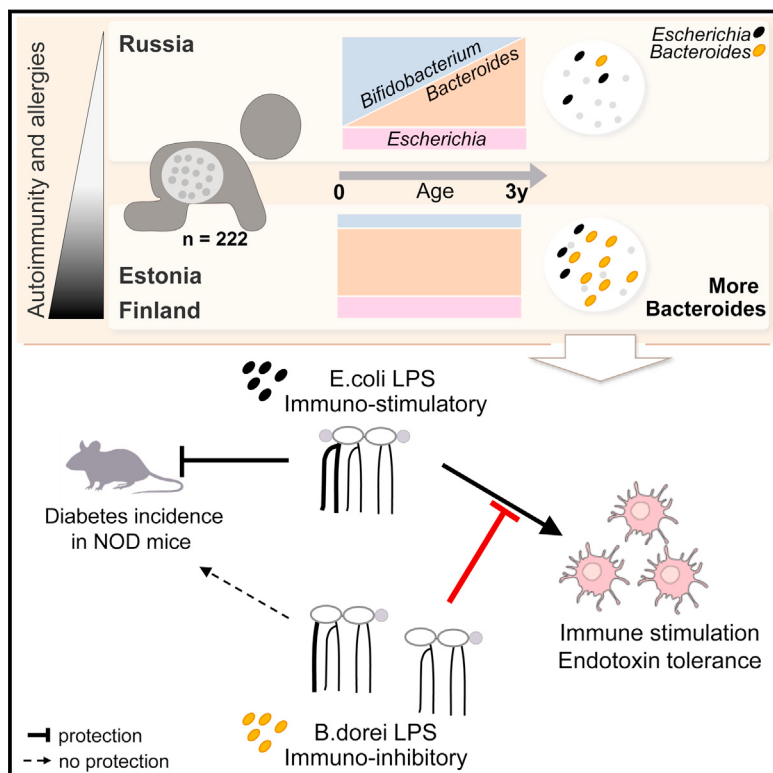


Variation in Microbiome LPS Immunogenicity Contributes to Autoimmunity in Humans

Graphical Abstract



Authors

Tommi Vatanen, Aleksandar D. Kostic,
Eva d'Hennezel, ..., Thomas W. Cullen,
Mikael Knip, Ramnik J. Xavier

Correspondence

xavier@molbio.mgh.harvard.edu

In Brief

Bacteroides species in the microbiota of children from countries with high susceptibility to autoimmunity produce a type of lipopolysaccharide (LPS) with immunoinhibitory properties. These properties may preclude early immune education and contribute to the development of type 1 diabetes.

Highlights

- Finnish and Estonian infants have a distinct early gut microbiome compared to Russians
- *B. dorei* and other *Bacteroides* species are highly abundant in Finland and Estonia
- *B. dorei* LPS inhibits the immunostimulatory activity of *E. coli* LPS
- LPS from *B. dorei* does not protect NOD mice from type 1 diabetes



Variation in Microbiome LPS Immunogenicity Contributes to Autoimmunity in Humans

Tommi Vatanen,^{1,2,22} Aleksandar D. Kostic,^{1,3,4,22} Eva d’Hennezel,^{5,22} Heli Siljander,^{6,7,8} Eric A. Franzosa,^{1,4} Moran Yassour,¹ Raivo Kolde,³ Hera Vlamakis,¹ Timothy D. Arthur,¹ Anu-Maria Hämäläinen,⁹ Aleksandr Peet,¹⁰ Vallo Tillmann,¹⁰ Raivo Uibo,¹¹ Sergei Mokurov,¹² Natalya Dorshakova,¹³ Jorma Ilonen,^{14,15} Suvi M. Virtanen,^{16,17,18} Susanne J. Szabo,⁵ Jeffrey A. Porter,⁵ Harri Lähdesmäki,² Curtis Huttenhower,^{1,4} Dirk Gevers,^{1,23} Thomas W. Cullen,^{5,23} Mikael Knip,^{6,7,8,19,23} on behalf of the DIABIMMUNE Study Group, and Ramnik J. Xavier^{1,3,20,21,23,*}

¹Broad Institute of MIT and Harvard, Cambridge, MA 02142, USA

²Department of Computer Science, Aalto University School of Science, 02150 Espoo, Finland

³Center for Computational and Integrative Biology, Massachusetts General Hospital and Harvard Medical School, Boston, MA 02114, USA

⁴Department of Biostatistics, Harvard School of Public Health, Boston, MA 02115, USA

⁵Novartis Institutes for Biomedical Research Inc., Cambridge, MA 02139, USA

⁶Children’s Hospital, University of Helsinki and Helsinki University Hospital, 00290 Helsinki, Finland

⁷Research Programs Unit, Diabetes and Obesity Research Program, University of Helsinki, 00290 Helsinki, Finland

⁸Department of Pediatrics, Tampere University Hospital, 33521 Tampere, Finland

⁹Department of Pediatrics, Jorvi Hospital, Helsinki University Hospital, 02740 Espoo, Finland

¹⁰Department of Pediatrics, University of Tartu and Tartu University Hospital, 51014 Tartu, Estonia

¹¹Department of Immunology, Institute of Biomedicine and Translational Medicine, Centre of Excellence for Translational Medicine, University of Tartu, 50411 Tartu, Estonia

¹²Ministry of Health and Social Development, Karelian Republic of the Russian Federation, Lenin Street 6, 185035 Petrozavodsk, Russia

¹³Petrozavodsk State University, Department of Family Medicine, Lenin Street 33, 185910 Petrozavodsk, Russia

¹⁴Immunogenetics Laboratory, University of Turku, 20520 Turku, Finland

¹⁵Department of Clinical Microbiology, University of Eastern Finland, 70211 Kuopio, Finland

¹⁶Department of Health, National Institute for Health and Welfare, 00271 Helsinki, Finland

¹⁷School of Health Sciences, University of Tampere, 33014 Tampere, Finland

¹⁸Science Centre, Pirkanmaa Hospital District and Research Center for Child Health, University Hospital, 33521 Tampere, Finland

¹⁹Folkhälsan Research Center, 00290 Helsinki, Finland

²⁰Gastrointestinal Unit and Center for the Study of Inflammatory Bowel Disease, Massachusetts General Hospital and Harvard Medical School, Boston, MA 02114, USA

²¹Center for Microbiome Informatics and Therapeutics, Massachusetts Institute of Technology, Cambridge, MA 02139, USA

²²Co-first author

²³Co-senior author

*Correspondence: xavier@molbio.mgh.harvard.edu

<http://dx.doi.org/10.1016/j.cell.2016.04.007>

SUMMARY

According to the hygiene hypothesis, the increasing incidence of autoimmune diseases in western countries may be explained by changes in early microbial exposure, leading to altered immune maturation. We followed gut microbiome development from birth until age three in 222 infants in Northern Europe, where early-onset autoimmune diseases are common in Finland and Estonia but are less prevalent in Russia. We found that *Bacteroides* species are lowly abundant in Russians but dominate in Finnish and Estonian infants. Therefore, their lipopolysaccharide (LPS) exposures arose primarily from *Bacteroides* rather than from *Escherichia coli*, which is a potent innate immune activator. We show that *Bacteroides* LPS is structurally distinct from *E. coli* LPS and inhibits innate immune signaling and endotoxin tolerance; furthermore, unlike LPS from *E. coli*, *B. dorei* LPS does not decrease incidence of autoimmune

diabetes in non-obese diabetic mice. Early colonization by immunologically silencing microbiota may thus preclude aspects of immune education.

INTRODUCTION

According to the hygiene hypothesis, early exposure to specific microorganisms and parasites in infancy benefits immune system development and confers protection against allergic and autoimmune diseases. Indeed, several studies have demonstrated a global gradient in the incidence of type 1 diabetes (T1D), multiple sclerosis, and other autoimmune diseases in association with improved sanitation and decreased incidence of early childhood infections (reviewed in Bach, 2002; Bach and Chatenoud, 2012). Similarly, rates of asthma and allergy are reduced in children exposed to a farm environment (von Mutius and Vercelli, 2010). One explanation for this effect posits that hygienic measures meant to prevent infectious disease by removing microbes from individuals’ living environments may, in turn, alter the indigenous intestinal microbiota, eliminating microbes important for educating the immune system (Bach, 2002; von Mutius and

Vercelli, 2010). Accordingly, studies in mouse models have shown that early colonization with a protective microbiota can diminish the risk of autoimmune diabetes development in genetically susceptible animals (Markle et al., 2013). Likewise, the composition of the microbiota can protect mice from allergies (Stefka et al., 2014). However, the distinction between beneficial and harmful microbial communities and the functional mechanisms underlying their effects are still poorly understood.

A microcosm of the global gradient in immune disease incidence occurs at the border between Finland and Russian Karelia, where there is a 2- to 6-fold higher incidence of allergies (Seiskari et al., 2007) and a 5- to 6-fold higher incidence of T1D and other autoimmune disorders (Kondashova et al., 2008a, 2008b) in Finland relative to Russian Karelia. In nearby Estonia, coinciding with economic development and improvement in living standards, the incidence of T1D and atopy has been transitioning in recent decades from rates similar to those of Russian Karelia toward those of Finland (Teeäär et al., 2010; Voor et al., 2005). Using these three populations as a “living laboratory,” the DIABIMMUNE study (<http://www.diabimmune.org/>) recruited a total of ~1,000 infants from Espoo (Finland), Petrozavodsk (Russia), and Tartu (Estonia). The infants were followed from birth to 3 years of age by monthly stool sampling along with collection of extensive clinical metadata. The cohort thus provides, to date, the largest longitudinal functional profile of the infant gut microbiome in relation to immune-mediated diseases, supplying an unprecedented opportunity to understand the microbial ecology and molecular mechanisms potentially underlying the hygiene hypothesis (Peet et al., 2012).

To characterize host-microbe immune interactions contributing to autoimmunity and allergy, we performed a longitudinal metagenomic characterization in 785 gut microbial communities from infants in the DIABIMMUNE cohort selected for this study (Figures 1A and 1B). Using strain-level microbial identification, we uncovered substantial differences in the composition, diversity, and stability of the early gut microbiome in Russian, Finnish, and Estonian children. We further quantified the functional potential of these microbial communities, stratifying gene families and pathways across their contributing organisms. This extensive dataset constitutes a valuable resource for infant gut microbiome investigations and is accessible through the DIABIMMUNE Microbiome Web site at <http://pubs.broadinstitute.org/diabimmune>.

In this work, we bridge deep human longitudinal metagenomic analysis with the identification of novel molecular immune mechanisms (Figure 1C). After extensive analysis of this dataset, we discovered that Finnish and Estonian infants harbored both a greater proportion of *Bacteroides* species and enrichment in lipopolysaccharide (LPS) biosynthesis-encoding genes, when compared to Russian infants. Our investigations revealed that these *Bacteroides* species produced a structurally and functionally distinct form of LPS; this LPS differed from the dominating form of LPS in the early Russian microbiome that was almost exclusively derived from *E. coli*. We further experimentally demonstrated that LPS from *Bacteroides dorei*, previously associated with T1D pathogenesis (Davis-Richardson et al., 2014), harbored tetra- and penta-acylated lipid A structures, as opposed to the hexa-acylated lipid A seen in *E. coli*. Furthermore, *B. dorei* LPS inhibited immune stimulation and inflammatory

cytokine responses to *E. coli* LPS in human cells. These findings suggest that differences in microbiota-derived LPS may preclude aspects of immune education in Finnish and Estonian children, uncovering one potential mechanism linking the human gut microbiome to susceptibility to immune diseases.

RESULTS

Study Cohort

A subcohort of 74 infants from each country was selected on the basis of similar histocompatibility leukocyte antigen (HLA) risk class distribution and matching gender (Figures 1A and 1B; Table S1). For each infant, 3 years of monthly stool samples and questionnaires regarding breastfeeding, diet, allergies, infections, family history, use of drugs, clinical examinations, and laboratory assays were collected. In accordance with the recruitment criteria for the DIABIMMUNE cohort, all subjects had increased HLA-conferred susceptibility to autoimmunity (Figure 1B) (Larizza et al., 2012; Sollid and Thorsby, 1993). Although these children were only followed until 3 years of age and it was therefore unlikely to see indications of allergic disease or autoimmunity, laboratory examinations revealed a high prevalence of allergen-specific sensitization and seropositivity for T1D-associated antibodies in Finnish and Estonian infants (Figure 1B, bottom).

We also observed a gradient in T1D autoantibody seropositivity within the cohort with higher prevalence of T1D autoantibodies in Finland. The number of infants that tested seropositive for one or more T1D-associated autoantibodies was 16 for Finland, 14 for Estonia, and 4 for Russia. Other studies in an older population (7–15 years of age) have shown that children in Russian Karelia display a substantially higher microbial exposure than their Finnish peers, as denoted by higher prevalence of antibodies against *Helicobacter pylori* (15-fold), *Toxoplasma gondii* (5-fold), and hepatitis A virus (12-fold) (Seiskari et al., 2007). This increased pathogen exposure in older children suggests an overall higher exposure rate to diverse microorganisms, possibly due to higher hygiene levels in urban Finland.

Regional Trends in the Gut Microbiota

To generate an overview of the composition of the gut microbiota throughout the first three years of life, we sequenced the V4 region of the 16S rRNA gene from 1,584 samples (Figure S1) and observed several strong high-level trends within this cohort. Principal coordinate plots (Figure 2A) showed that, besides age, country was the major source of variation, particularly during the first year of life. To further confirm separability between countries, we trained a set of random forest classifiers using genus-level data from samples collected between 170 and 260 days of age. The classifier was able to predict country with high-classification accuracy (area under the curve [AUC] = 0.944 for Finns versus Russians) (Figure 2B). Classification was least accurate between Finns and Estonians (AUC = 0.546), suggesting that early microbial profiles were fairly homogenous in these two countries. Differences between the Russian samples compared to Finnish and Estonian samples were already evident at phylum-level composition (Figure 2C), represented by two distinct hallmarks. First, Finnish and Estonian children had higher

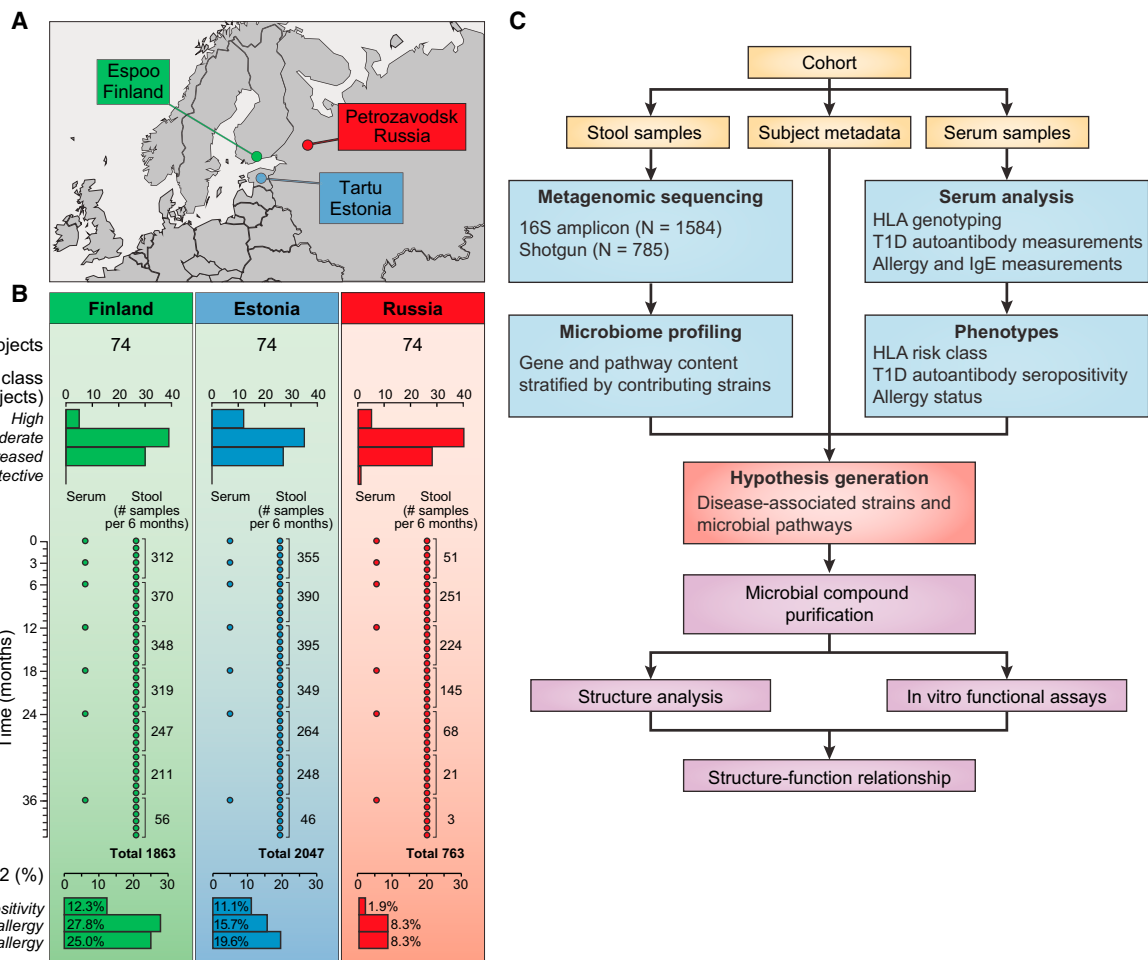


Figure 1. DIABIMMUNE Cohort

(A) Locations of cities and countries in which DIABIMMUNE infants were screened and samples were collected.

(B) Selected within-cohort statistics and stool sample collection schedule (monthly stool sampling until three years of age). Numbers next to stool samples reflect the number of samples collected in 6-month time windows. Within-cohort distribution of HLA conferred risk for autoimmunity is shown (see Table S1 for corresponding HLA allele identities), as well as prevalence of T1D-associated autoantibody seropositivity, egg allergy, and milk allergy at year 2. For T1D autoantibody seropositivity, n = 291 serum samples from 73 infants for Finns, n = 235 serum samples from 72 infants for Estonians, and n = 118 serum samples from 54 infants for Russians. For egg allergy, n = 72 for Finns, n = 51 for Estonians, and n = 24 for Russians. For milk allergy, n = 72 for Finns, n = 46 for Estonians, and n = 24 for Russians.

(C) Analysis workflow highlighting important steps in metagenomic data analysis and mechanistic experiments.

See also Figure S1 and Table S1.

levels of Bacteroidetes throughout the 3-year period (false discovery rate [FDR] corrected $p = 5.4 \times 10^{-15}$; see the [Supplemental Experimental Procedures](#)). Second, Russians had higher levels of the phylum Actinobacteria during the first year of life (FDR corrected $p = 0.014$). The latter difference dissipated over time and was no longer significant after two years of age. The abundance of the phylum Bacteroidetes correlated with serum insulin autoantibody (IAA) levels, both within Finland ($p = 0.017$) and cohort-wide ($p = 0.0020$; [Figure S2](#); [Supplemental Experimental Procedures](#)). We conducted extensive testing of associations between the metadata and taxonomic groups using MaAsLin, a linear modeling tool adapted for microbial community data ([Morgan et al., 2012](#)). Hence, all reported country-level differences were corrected for all major confounding effects,

such as birth mode, breastfeeding and other dietary factors, antibiotics use, and age (see the [Supplemental Experimental Procedures](#)). [Table 1](#) highlights selected associations between the metadata and microbiota. A comprehensive list of results, including taxonomic differences between countries, taxonomic alterations associated with allergen-specific immunoglobulin E (IgE), and microbial changes associated with other collected metadata, can be accessed at <http://pubs.broadinstitute.org/diabimmune>.

The diversity of the microbiota within individual samples (alpha diversity) increased with age ([Figure S3A](#)) as the microbiota developed toward an adult composition ([Koenig et al., 2011](#)). However, Russians displayed a significantly less diverse microbiota compared to Finns and Estonians during the first

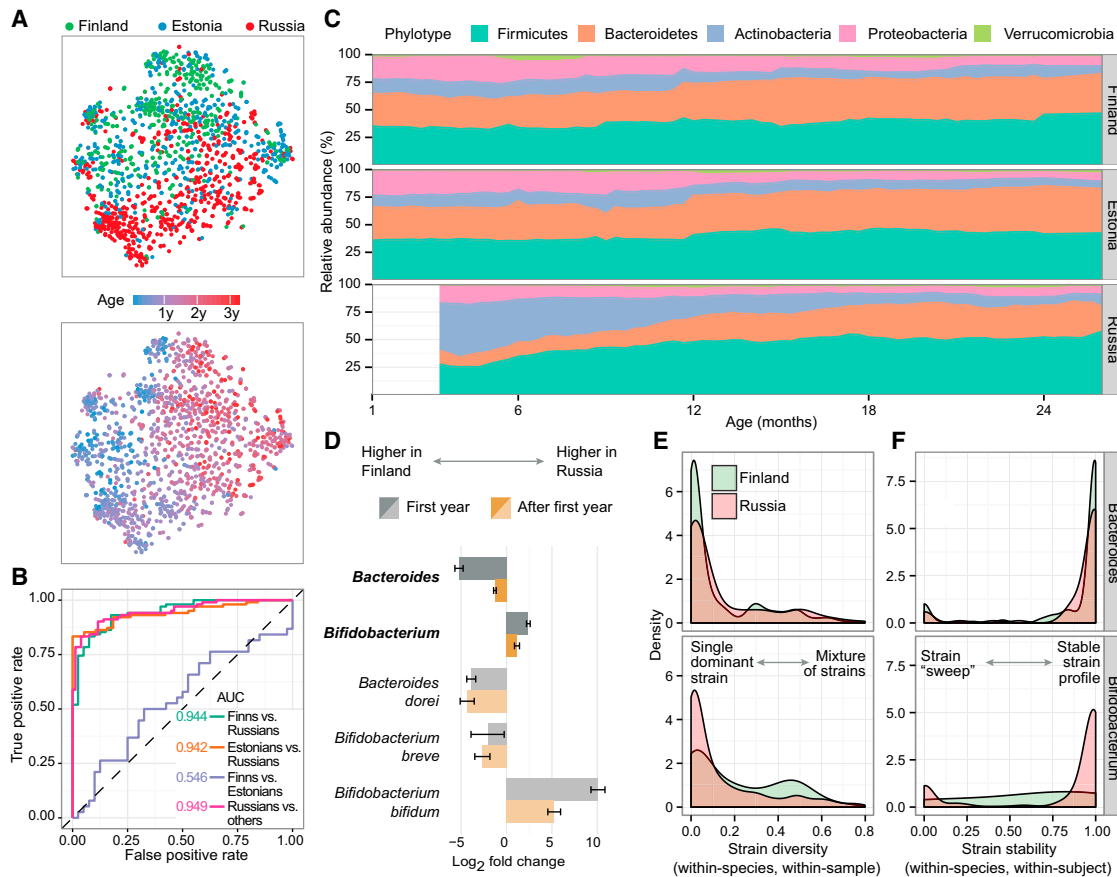


Figure 2. Differences in Microbial Ecology between Countries in Early Infancy

(A) Principal coordinate analysis plots of DIABIMMUNE 16S samples, colored by country (top) and age (bottom). Each circle represents an individual stool sample ($n = 1,584$).

(B) ROC curves for pairwise random forest classifiers predicting country based on 16S genus data using samples collected between 170 and 260 days of age.

(C) Average phylum-level composition of DIABIMMUNE samples during the first 2 years of age.

(D) Genus-level (darker colors) and species-level (lighter colors) bootstrapped mean \log_2 fold changes and their SD between Finnish and Russian gut microbiota during the first year and after.

(E and F) Strain-level diversity (E) and stability (F) in *Bacteroides* and *Bifidobacterium* species. Diversity and stability distributions for *Bifidobacterium* species are significantly different between the Finnish and Russian populations (two-sample Kolmogorov-Smirnov test; $p = 5.0 \times 10^{-4}$ and $p = 1.5 \times 10^{-6}$, respectively). See also Figures S2, S3, and S4.

year (Figure S3B). This difference could be explained by the 2-fold overrepresentation of the phylum Actinobacteria and the genus *Bifidobacterium* in the Russians for that time period (Figures 2C and 2D). Lastly, we also uncovered differences in stability within taxa between the countries. These differences were particularly evident when comparing samples collected during early and late time windows (Figures S3C and S3D). Russians had an overall more plastic microbiota during the first 3 years of life, with the exception of the most dominant genus *Bifidobacterium* in the early time window. In contrast, the phylum Bacteroidetes and the genus *Bacteroides* were more stable in Finns and Estonians throughout the entire observation period. Taken together, we uncovered strong global differences between the Russian versus Finnish and Estonian microbiota, with the largest differences occurring in the first year and dissipating during the second and third years.

Species- and Strain-Level Microbial Dynamics

To obtain a more complete and higher resolution taxonomic view of the infants' microbiome, we performed deep whole-genome shotgun metagenomic sequencing on a representative subset of 785 samples (Figure S1). We first investigated the metagenomic reads for their detailed taxonomic composition down to the species level using MetaPhlAn (v.2.2) (Metagenomic Phylogenetic Analysis) (Truong et al., 2015) and observed multiple differentially abundant species in the *Bacteroides* and *Bifidobacterium* genera between Finland and Russia (Figure 2D). Notably, *B. dorei*, which has been previously associated with T1D pathogenesis (Davis-Richardson et al., 2014), was the *Bacteroides* species with the largest fold change between Finns and Russians. We confirmed the validity of the metagenomics data by running qPCR on DNA from 85 stool samples. Interpolated absolute abundances of *B. dorei* and *E. coli* species were in good agreement with absolute abundances predicted by the

Table 1. Associations between Metadata and Microbiota

	Increased	Decreased
T1D AAB seropositivity	<i>Rothia</i> (g) <i>Gemellaceae</i> (f)*	<i>Bilophila</i> (g)* <i>Sutterella</i> (g)*
Cesarean section	<i>Firmicutes</i> (p)** <i>Eubacterium</i> (g)** <i>Ruminococcus</i> (g)*	<i>Bacteroidetes</i> (p)** <i>Bacteroides</i> (g)** <i>Faecalibacterium prausnitzii</i> *
Antibiotics	<i>Deltaproteobacteria</i> (c)* <i>Bilophila</i> (g)*	<i>Gammaproteobacteria</i> (c)** <i>Clostridium</i> (g)** <i>Haemophilus</i> (g)**
Breastfeeding	<i>Actinobacteria</i> (p)** <i>Bifidobacterium</i> (g)** <i>Lactobacillus</i> (g)**	<i>Blautia</i> (g)** <i>Oscillospira</i> (g)**
Baby formula	<i>Citrobacter</i> (g)** <i>Veillonella</i> (g)	<i>Streptococcus</i> (g)
Cow's milk	<i>Lactococcus</i> (g)** <i>Collinsella</i> (g)** <i>Lactococcus lactis</i>	<i>Staphylococcus</i> (g)
Wheat	<i>Bifidobacterium pseudocatenulatum</i> **	<i>Staphylococcus</i> (g)**
Barley	<i>Betaproteobacteria</i> (c)** <i>Sutterella</i> (g)**	
Oat	<i>Lachnospiraceae</i> (f)** <i>Clostridium bartletti</i> *	<i>Enterobacteriales</i> (o)**
Corn	<i>Blautia</i> (g)**	<i>Ruminococcaceae</i> (f)
Rice	<i>Epsilonproteobacteria</i> (c)** <i>Prevotella</i> (g)*	
Eggs	<i>Cyanobacteria</i> (p)* <i>Ruminococcus</i> (g)** <i>Lactococcus</i> (g)	
Vegetables	<i>Clostridia</i> (c) <i>Lachnospiraceae</i> (f)**	<i>Holdemania</i> (g)**
Root vegetables	<i>Ruminococcus</i> (g)** <i>Coprococcus catus</i> **	<i>Betaproteobacteria</i> (c) <i>Bacteroides</i> (g)
Meat	<i>Proteobacteria</i> (p) <i>Erysipelotrichaceae</i> (f)** <i>Bacteroides</i> (g)*	<i>Firmicutes</i> (p)** <i>Coprococcus</i> (g)**
Fish	<i>Parabacteroides</i> (g)	
Soy	<i>Alphaproteobacteria</i> (c)** <i>Lachnospira</i> (g)* <i>Clostridium clostridioforme</i>	<i>Holdemania</i> (g)**

The table shows microbial taxa that are associated with T1D autoantibody seropositivity, caesarean section, intake of antibiotics, breastfeeding, and other dietary compounds. The left column shows taxa that are increased, and the right column shows taxa that are decreased in each association. All findings are FDR-corrected; p < 0.1, *p < 0.01, **p < 0.001. p, phylum; c, class; o, order; f, family; g, genus.

See also the [Supplemental Experimental Procedures](#) and <https://pubs.broadinstitute.org/diabimmune/three-country-cohort/resources/metadata-association-analysis>.

metagenomics data when total bacterial mass was estimated using universal 16S primers ([Figure S3E](#); [Supplemental Experimental Procedures](#)).

Next, we analyzed the metagenomics data at the strain level using ConStrains, a recently developed strain haplotyping tool, and evaluated the diversity and stability of the infant microbiota ([Luo et al., 2015](#)). In 60% of all strain profiles, communities were composed of species with a single dominant strain (>90% within-species abundance), as reflected in low within-species, within-sample haplotype diversity scores ([Figure S4A](#)). However, species in some genera, such as *Faecalibacterium* and *Veillonella*, had bimodal haplotype diversity distributions, indicative of more complex strain compositions. Moreover, strain diversity had a tendency to increase with age ([Figure S4B](#)). Analysis of the strain stability over time revealed that species tended to either (1) remain stable, maintaining their single dominant strain, or (2) experience a strain “sweep,” in which the original dominant strain was replaced by a new dominant strain ([Figure S4C](#)). We observed an inverse correlation between the longitudinal distance of the samples and the corresponding strain stability ([Figure S4D](#)). When comparing strain stability with average diversity of the compared samples, we saw an inverse correlation, indicating that less diverse strain profiles (i.e., single dominant strain behavior) tended to be more stable compared to more diverse strain profiles ([Figure S4E](#)). Within the genera of interest, we observed that *Bifidobacterium* species failed to establish stable single-strain communities in Finnish children, as shown by a more evenly distributed strain diversity and stability compared to Russians ([Figures 2E](#) and [2F](#)). In contrast, *Bacteroides* species (when present) tended to establish stable, single-strain compositions in both Finns and Russians ([Figures 2E](#) and [2F](#)).

Differential Microbial Functions between Populations

To survey the functional and metabolic consequences of the taxonomic differences between countries, we next analyzed the metagenomic sequences for their genomic functional potential using HUMAnN2 ([Abubucker et al., 2012](#)) and linked quantified gene abundances (reads per kilobase per million reads [RPKMs]) to gene ontology (GO) terms. As observed for microbial diversity, functional diversity of the microbiome also started with a less complex composition in Russians but developed to reach greater diversity by the end of the 3-year period ([Figure S5A](#)). We identified multiple GO categories with significantly different abundances between Finns and Russians in both the early (first year) and late (after first year) time windows ([Figure 3A](#)). For instance, siderophore-related functions, which include iron scavenging, as well as virulence-related functionalities, were higher in Finnish infants, possibly reflecting an increase in pathobiont organisms in Finland. A comprehensive list of differential categories between the two countries is shown in [Figure S5B](#) and [Table S2](#).

Glycolytic functions were differentially abundant between the two populations ([Figure 3A](#)), leading us to computationally investigate differences in milk oligosaccharide metabolism. The gut microbiome composition within the first year is largely shaped by milk, the sole nutrient source available to infants, whether from breast- or bottle-feeding (reviewed in [Sela and Mills, 2010](#)). The *Bifidobacterium* and *Bacteroides* genera are

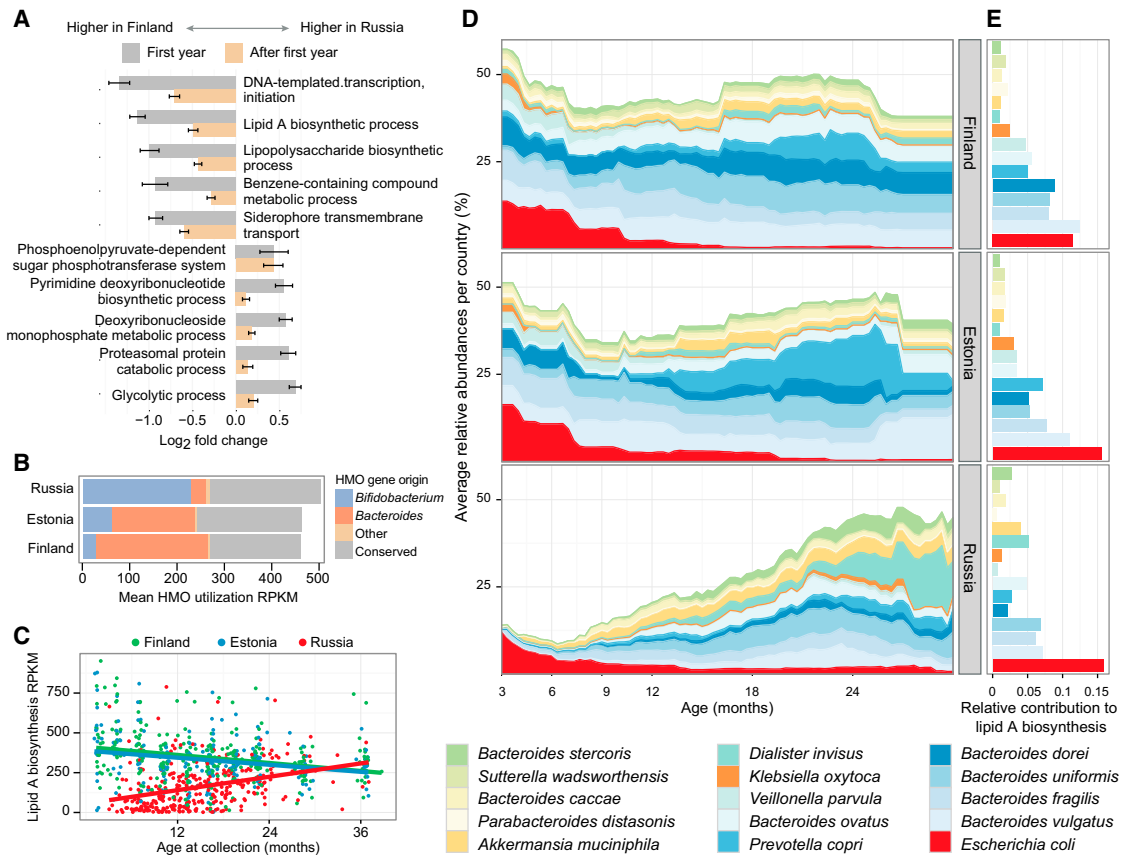


Figure 3. Functional Differences, HMO Utilization, and Lipid A Biosynthesis

(A) Bootstrapped mean log₂ fold changes and their SD in the functional categories with the largest differences between Finnish and Russian children.

(B) Mean human milk oligosaccharide utilization gene abundance across the three countries within the first year of life, stratified by taxonomic origin of each gene (“conserved” genes were too highly conserved to confidently assign to a unique genus).

(C) Lipid A biosynthesis pathway normalized read counts (RPKM) per sample ($n = 785$) and a linear fit per country.

(D and E) Mean relative abundances of 15 species with the largest contributions to the lipid A biosynthesis signal (D) and their relative contributions (E) to the signal in all samples within each country.

See also Figure S5 and Table S2.

the two main groups of human milk oligosaccharide (HMO)-metabolizing bacteria (Marcobal et al., 2011). Within *Bifidobacterium*, *B. bifidum* and *B. longum* (predominant in Russians) are capable of metabolizing HMOs, whereas *B. breve* (present in Finns) is incapable of metabolizing intact HMOs, though it readily utilizes monosaccharides liberated from HMOs (Locascio et al., 2009). This observation led us to hypothesize that HMO metabolism in Finnish and Estonian children is performed by *Bacteroides* species, whereas it is performed by *B. bifidum* and *B. longum* in Russians. Indeed, by analyzing the taxonomic origin of genes belonging to a bona fide HMO gene cluster (Sela et al., 2008), we showed that although the average abundance of HMO utilization genes is approximately equal across the three countries (mean \pm SD in RPKM: Finland 460 ± 372 , Estonia 462 ± 331 , Russia 504 ± 469), most of the genes are conferred by *Bifidobacterium* in Russians and *Bacteroides* in Finns and Estonians (Figures 3B and S5C). We note that the higher abundance of *B. bifidum* in Russians is not a result of increased breastfeeding; Finnish infants were breastfed for a longer period

than Russians, on average (mean \pm SD breastfeeding/days: Finland 268 ± 149 , Estonia 307 ± 217 , Russia 199 ± 165).

Most significantly, we found that GO terms related to LPS functions, LPS biosynthetic process (GO: 0009103), and lipid A biosynthetic process (GO: 0009245) showed a striking difference in abundance between countries (Figures 3A and 3C), indicating that microbial communities in Finnish and Estonian subjects produced more LPS. This molecule is of particular interest because it elicits a strong immune response in mammalian cells (Cullen et al., 2015). When deconvoluting the species contributing to biosynthesis of lipid A, the subunit responsible for the immunostimulatory properties of LPS, we made two key observations. In all three countries, *E. coli* was a major contributor to lipid A biosynthesis, but in Finland and Estonia a number of other bacterial species contributed to lipid A biosynthesis potential, many of which belong to the genus *Bacteroides* (Figures 3D and 3E). LPS subtypes derived from *Bacteroides* species have been shown to exhibit lower endotoxicity relative to LPS isolated from other enteric bacteria (Hofstad et al., 1977). This finding

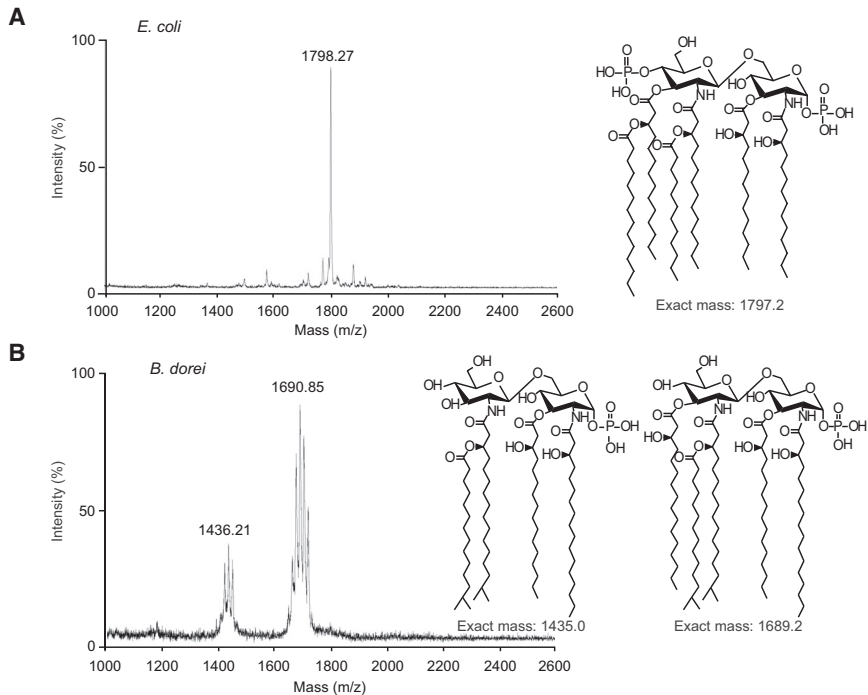


Figure 4. Structures of LPS Molecules and Impact on Tolerogenic Function

(A and B) MALDI-TOF MS analysis of lipid A purified from *E. coli* (A) and *B. dorei* (B). Representative structures are shown as insets with predicted exact mass.

See also Figure S6 and Table S3.

LPS structural analysis. These data revealed identical LPS structural features across all *B. dorei* isolates (Figures S6A and S6B). Thus, our findings regarding *B. dorei* LPS structure and function are likely to be recapitulated in patients.

Extensive lipid A structure-function studies have shown that the number of acyl chains is a strong determinant of immune activation by LPS (Hajjar et al., 2002; Needham et al., 2013) and that penta- and tetra-acylated lipid A structures elicit reduced TLR4 responses (Herath et al., 2011). In order to understand the consequences of the structural differences between the LPS subtypes, we assessed the immunogenicity of LPS

prompted us to examine whether there was a difference in immunogenicity of the LPS subtypes derived from the predominant species of the three populations.

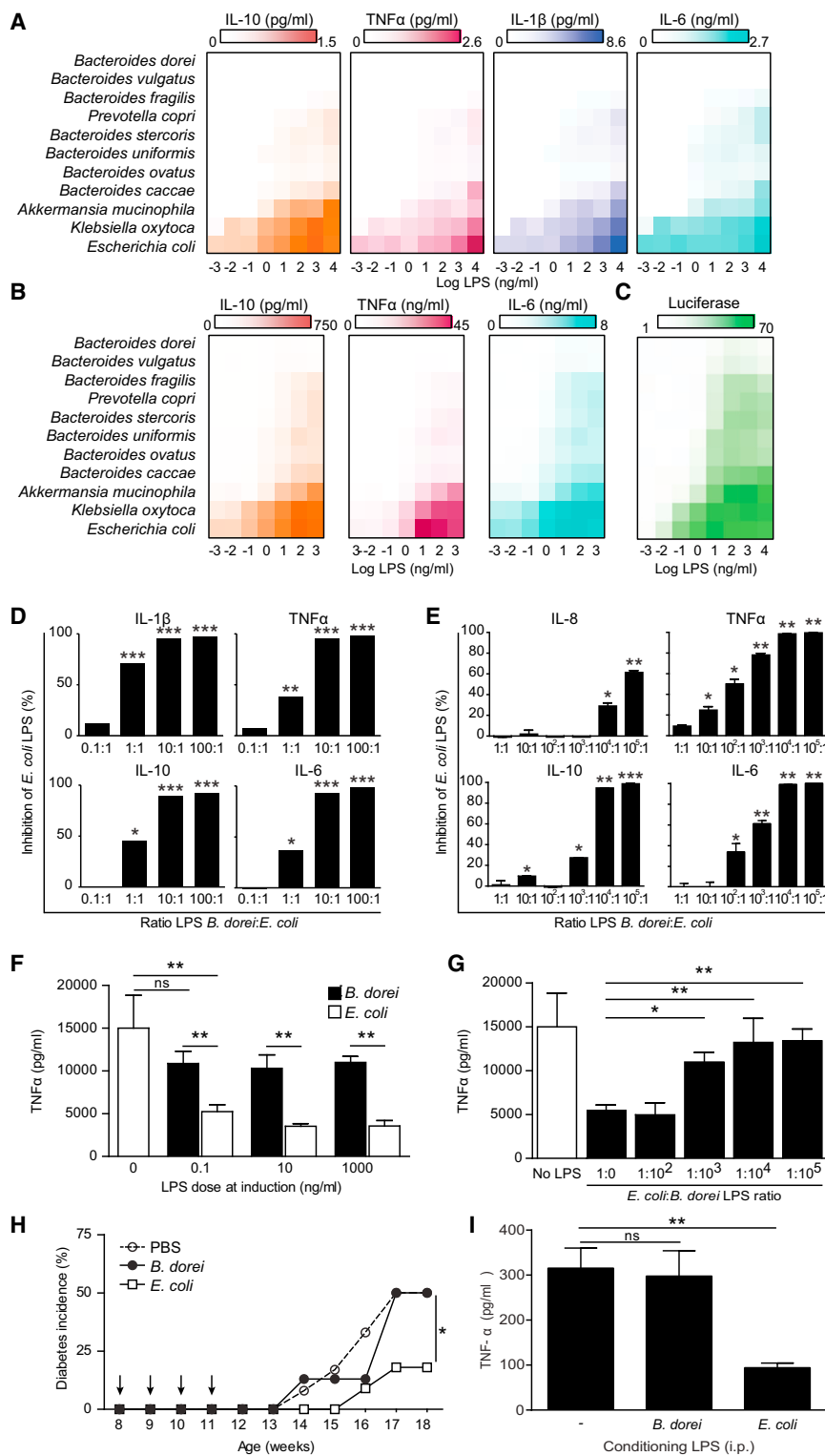
Contrasting Immunogenicity of LPS Subtypes

Inter-species differences in LPS structure are associated with alterations in their capacity to elicit an innate immune response (Whitfield and Trent, 2014). Specifically, the lipid A domain of LPS is responsible for immune signaling through recognition and activation of the Toll-like receptor 4 (TLR4) complex (Kim et al., 2007); as such, structural changes in lipid A impact recognition by TLR4 and influence multiple facets of microbial ecology (Cullen et al., 2015; Whitfield and Trent, 2014). We purified LPS (see below) and used matrix-assisted laser desorption/ionization-time of flight mass spectrometry (MS) to examine the structure of the lipid A domain of two bacterial species (type strains): *E. coli* as a representative of the most common immunostimulatory lipid A structure and *B. dorei*, which was the most differentially abundant *Bacteroides* species between the countries (Figures 2D and 3D). Lipid A extracted from *E. coli* produced a predominant peak at a mass-to-charge ratio (*m/z*) of 1798.3, consistent with the published [M-H]⁻ ion structure of *E. coli* lipid A (Needham et al., 2013) carrying two phosphate groups and six acyl chains (predicted exact mass: 1,797.2 *m/z*) (Figure 4A). Lipid A extracted from *B. dorei* produced two predominant peaks at *m/z* 1,690.9 and 1,436.2, consistent with the [M-H]⁻ ion structures with one phosphate group and four and five acyl chains, respectively (predicted exact mass: 1,689.2 and 1,435.0 *m/z*) (Figure 4B).

In order to ensure that LPS from our *B. dorei* type strain was representative of clinical samples, we isolated *B. dorei* strains from stool samples of six healthy donors for comparative

derived from the bacterial species contributing to the LPS load in our samples (see Figure 3E). Of the 15 strongest contributors, we were able to purify LPS from 11 type strains listed in Table S3. We first used the LPS purified from these strains to stimulate primary human peripheral blood mononuclear cells (PBMCs), which contain LPS-responsive cell types similar to those present in the gut and are thus a common proxy for mucosal leukocytes (Ardesir et al., 2014; Sokol et al., 2008). LPS derived from *E. coli* produced a strong response as measured by the production of the necrosis factor κ B (NF- κ B)-dependent cytokines interleukin-10 (IL-10), tumor necrosis factor alpha (TNF α), IL-1 β , and IL-6 in primary PBMCs (Figures 5A and S7A), whereas LPS derived from *B. dorei* failed to elicit any response regardless of the dose. Notably, LPS derived from all analyzed members of the phylum Bacteroidetes (*Bacteroides* species and *Prevotella copri*) also showed a severely impaired capacity to elicit the production of these inflammatory cytokines. We then measured cytokine production in human monocyte-derived dendritic cells after stimulation with LPS from these same strains and obtained similar results (Figures 5B and S7B). Consistent with assays in primary cells, *E. coli*-derived LPS elicited high levels of luciferase activity in TLR4-NF- κ B reporter cells, whereas *Bacteroides* species failed to induce an inflammatory signal in these cells (Figures 5C and S7C).

Our metagenomics analyses revealed that *E. coli* and *B. dorei* LPS often co-occur in the gut of Finnish and Estonian infants. In order to study possible interactions between these LPS subtypes, we used a base dose of *E. coli* LPS, while co-treating human primary immune cells with *B. dorei* LPS at increasing ratios. We then measured changes in the production of inflammatory cytokines with respect to baseline *E. coli* LPS stimulation. Cytokine production was inhibited by *B. dorei* LPS in primary human



PBMCs (Figure 5D) and in monocyte-derived dendritic cells (Figure 5E). Notably, we observed maximal inhibition in PBMCs at a ratio of 10:1 *B. dorei*:*E. coli* LPS, corresponding to the

Figure 5. Immunostimulatory Properties of LPS from Different Bacterial Strains

(A) Mean cytokine production in PBMCs stimulated with the indicated doses of LPS as assessed by cytokine bead array.

(B) Mean cytokine production in monocyte-derived dendritic cells stimulated with indicated doses of LPS.

(C) Reporter cells expressing human TLR4 were stimulated with LPS from different bacterial strains for 6 hr, and NF-κB activity was measured by luciferase activity. Activity is expressed as the percent of maximum luciferase signal.

(D and E) Inhibition of *E. coli* LPS-induced PBMC

(D) or monocyte-derived dendritic cells (E) cytokine production by additional doses of LPS from *B. dorei*. Inhibition of cytokine production is shown in comparison to stimulation with *E. coli* LPS alone.

(F) Induction of endotoxin tolerance by LPS from *E. coli* or *B. dorei* in primary human monocytes as assessed by cytokine bead array. Bars show TNF α concentration in monocyte supernatants after 24-hr restimulation with zymosan as assessed by cytokine bead array.

(G) Inhibition of *E. coli*-driven endotoxin tolerance induction in human monocytes by *B. dorei* LPS.

(H) Impact of *E. coli*- or *B. dorei*-derived LPS exposure on diabetes incidence in NOD mice. Mice were injected i.p. once a week (arrows) with LPS from *E. coli* ($n = 9$ mice) or *B. dorei* ($n = 12$ mice). Blood glucose was monitored weekly.

(I) Induction of endotoxin tolerance in NOD mice. The mice ($n = 5$ per group) were injected i.p. with LPS purified from *E. coli* or *B. dorei*. The splenocytes were isolated after 24 hr and restimulated in vitro with zymosan. Bars show TNF α concentration assessed by cytokine bead array after 24 hr.

In vitro data are representative of three or more independent experiments and are presented as the mean (and SD) of triplicate assessments. * $p < 0.05$, ** $p < 0.005$ by Student's t test compared to *E. coli* stimulation (D and E), *E. coli* LPS treatment alone (F and G), or PBS treatment (I) or by ANOVA for diabetes incidence (H).

See also Figure S7.

computational prediction of the ratio between inhibitory and stimulatory LPS typical for IAA-seropositive infants (Figure S2). Similar to cytokine production in PBMCs, NF-κB-luciferase activity was inhibited by *B. dorei* LPS in a dose-dependent manner (Figure S7D). We also obtained similar results when examining cord blood mononuclear cells (Figures S7E and S7F), suggesting that our observations reflect the reaction of the naive immune system of infants. Our results show that *B. dorei* LPS acts as an inhibitor of immune stimulation by *E. coli*-derived LPS, with a potency that is concordant with ratios of the LPS subtypes observed in vivo.

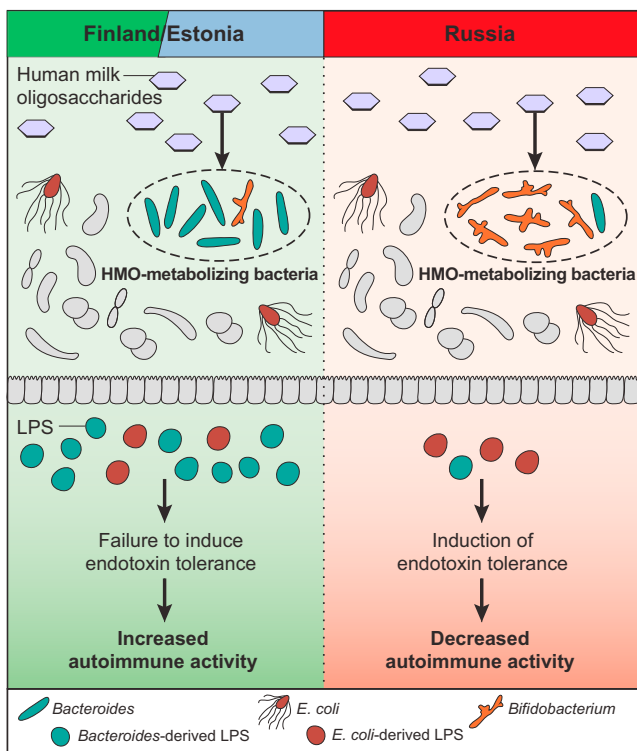


Figure 6. Differences in HMO-Utilizing Bacteria Provide a Route to Differences in Immune Education

Human milk oligosaccharides can be metabolized by different prevalent microbes in Russia (primarily *Bifidobacterium* species) versus Finland and Estonia (primarily *Bacteroides* species). Potentially as a result of these population differences, *Bacteroides*-derived lipopolysaccharide (LPS) constitutes the major portion of LPS produced by microbes in Finnish and Estonian infants, whereas LPS in Russian infants is mostly derived from *E. coli*. *Bacteroides*-derived LPS is of an immunoinhibitory subtype, thus leading to differential immune education by means of endotoxin tolerance or other routes.

It has been proposed that lipid A phosphorylation pattern contributes to LPS immunogenicity. However, LPS from a mutant strain of *B. thetaiotaomicron* (Δ LpxF), whose lipid A structure is identical to that of *B. dorei* but harbors two phosphate groups similar to *E. coli* (Cullen et al., 2015), did not increase LPS immunogenicity or alter its inhibitory capacity (Figures S7G and S7H). This suggests that lipid A phosphorylation status is unlikely to be the underlying mechanism of our observations.

Stimulation of immune cells with LPS induces a temporary refractory state to a repeated immune challenge, a phenomenon known as endotoxin tolerance (Watson and Kim, 1963). This mechanism of immunosuppression was originally described in sepsis, but is thought to underlie multiple other physiological contexts of innate immune unresponsiveness, such as the immune protective effect conferred by microbial exposure suggested by the hygiene hypothesis (Biswas and Lopez-Collazo, 2009). We assessed the potency of *E. coli* and *B. dorei* LPS subtypes to induce endotoxin tolerance in primary human monocytes. Initial exposure to *E. coli* LPS prevented TNF α production after restimulation at all conditioning doses tested (Figure 5F). In contrast, *B. dorei* LPS conditioning did not abrogate cytokine

production in these cells even at the highest concentrations, corresponding to a potency at least four orders of magnitude lower than *E. coli* LPS. Hence, the LPS produced by *B. dorei* failed to induce protective endotoxin tolerance. Finally, the addition of *B. dorei* LPS to *E. coli* LPS during the endotoxin tolerance induction phase prevented the establishment of endotoxin tolerance by *E. coli* LPS in a dose-dependent manner (Figure 5G), suggesting that the presence of *B. dorei* in the infant gut could prevent the establishment of protective immune tolerance by *E. coli* LPS.

To demonstrate the relevance of LPS-driven immune suppression in the development of autoimmunity in vivo, we assessed the impact of different LPS subtypes on diabetes development in the non-obese diabetic (NOD) mouse model of T1D. Intraperitoneal (i.p.) injection of *E. coli* LPS resulted in a delayed onset and reduced overall incidence of disease, as measured by blood glucose levels (Figure 5H). In contrast, *B. dorei* LPS did not delay the onset of diabetes and did not decrease incidence compared to the mock-injected group (PBS). Interestingly, as shown in Figure 5I, we also found that splenocytes isolated from NOD mice 24 hr after i.p. *E. coli* LPS injection were hyporesponsive to further in vitro innate immune stimulation, whereas *B. dorei* LPS did not alter the response. This shows that *E. coli* LPS, but not *B. dorei* LPS, can induce endotoxin tolerance in vivo in NOD mice. These results suggest that exposure to immunostimulatory LPS can contribute to protection from immune-mediated diseases by modulating the immune system responsiveness.

DISCUSSION

A growing body of evidence suggests that the gut microbiome may be a key factor in influencing predisposition to autoimmunity and allergic diseases. Here, we characterized infant gut microbiome development between three environmentally disparate populations and identified marked differences between these populations in the prevalence of important intestinal microbes, such as *Bifidobacterium* and LPS-producing *Bacteroides* species (Figure 6). Subsequently, we identified lipid A biosynthesis as one of the most differentially abundant functional pathways between the populations, suggesting that early microbial communities in Finnish and Estonian subjects produce more LPS compared to their Russian counterparts. Additionally, we uncovered functional and structural differences in the dominant microbial LPS subtypes. Notably, we showed that LPS produced by different constituents of the human gut microbiome could either stimulate or actively inhibit TLR4, NF- κ B activation, and endotoxin tolerance. Hence, rather than the mere amount of LPS, the nature and composition of different LPS subtypes seem to determine the level of immune activation triggered by the microbe-derived LPS cocktail. Importantly, we show that injection of an immunogenic subtype of LPS from *E. coli* can both elicit endotoxin tolerance in vivo in NOD mice and decrease the incidence of diabetes in these mice. These effects were not observed with LPS from *B. dorei*. Our observations suggest that microbiome-derived LPS could impact long-term immunosuppressive mechanisms in more complex ways than has been previously appreciated.

In the absence of specific biomarkers, we cannot determine what impact the differences in early LPS exposure has had in

Russian and Finnish infants in our cohort. However, the proposition of a direct impact of LPS on the pathophysiology of T1D is further supported by previous studies in mice. For example, Wen et al. (2008) have demonstrated that components of the microbiome modulate immune system activity, resulting in altered disease development in NOD mice. In addition, LPS has a direct impact on T1D progression in NOD mice by i.p. injection (Aumeunier et al., 2010) and oral gavage (Saï and Rivereau, 1996). The impact of the microbiome on T1D onset and development in NOD mice is dependent on TLR4 and MyD88, critical components of the LPS/TLR4 signal transduction pathway (Gülden et al., 2013; Wen et al., 2008). Taken together, these studies support a model whereby exposure to different LPS subtypes produced by the gut microbiome can contribute to immune modulation and alter the course of autoimmunity.

One limitation of mouse studies is that LPS subtypes that are antagonistic or silent in humans are instead recognized as stimulatory in mice due to differences between the mouse and human LPS co-receptor MD2 (Hajjar et al., 2002). However, our observation that mice react to *E. coli* LPS, but not to *B. dorei* LPS, suggests that the non-immunogenicity of *B. dorei* LPS is possibly independent of MD2 in both species. The specific mechanism of the antagonism mediated by *B. dorei* LPS in humans remains to be explored.

This study achieved a deep-level understanding of microbial community establishment in three different infant populations. Our analyses revealed a lengthy list of associations between microbial taxa and the rich metadata collected in the DIABIMMUNE study, such as dietary information, mode of delivery, and the use of antibiotics (see Table 1). A comprehensive list of our findings, including microbial alterations relative to allergen-specific IgE and T1D autoantibody seropositivity, containing numerous potentially interesting features of microbiota, can be found at <http://pubs.broadinstitute.org/diabimmune>.

Our analysis more broadly exercises a generalizable discovery and validation process for identifying and characterizing bioactive microbial products from the microbiome (Figure 1C). We began by identifying differentially abundant microbial processes between phenotypically distinct populations, assigned them to specific microbes, and, ultimately, identified structural differences within these pathways (e.g., LPS) that induced distinct immune responses in vitro. We targeted LPS biosynthesis for initial mechanistic follow-up because it was among the strongest signals and has a well-established connection to immune activation. This can be expanded in the future, since our study population included many additional functional differences in the gut, ranging from microbial metabolism (e.g., glycolysis) to iron uptake.

We found that HMO metabolism was a potential factor in establishing and/or maintaining a *Bifidobacterium*-dominant versus *Bacteroides*-dominant gut microbiota in the first year of life, likely because the two genera compete for HMOs as a common energy source (Marcobal et al., 2011). A significant role for HMO metabolism in determining microbial community composition is consistent with the hygiene hypothesis, given that mothers are also under environmental stress and can transfer these effects to their infants. In vaginal births, most of the early infant gut colonizers are derived from the mother's gut (Bäckhed

et al., 2015) and possibly consolidated by the microbiome in breast milk (Hunt et al., 2011). Transcriptomic analysis of cord blood from the infants in this cohort revealed a signal resembling the response to LPS exposure, suggesting that these infants are exposed to environmental stresses even before birth (Kallionpää et al., 2014).

The effects of the hygiene hypothesis are most likely mediated through not just one mechanism but rather a complex interplay of environmental factors. These likely include immune responses to multiple different parasites, helminths, microbes, and viruses. Here, we have identified one potential contributing factor, namely, immunogenicity of early colonizing symbiotic bacteria. Understanding how the different members of our microbiota contribute to the development of our immune system alone and in combination will be a key step in the development of probiotic interventions that may alter the increasing trends of autoimmune diseases in countries such as Finland.

EXPERIMENTAL PROCEDURES

Study Cohort

The international DIABIMMUNE study recruited 832 families in Finland (Espoo), Estonia (Tartu), and Russia (Petrozavodsk) with infants carrying HLA alleles that conferred risk for autoimmunity (Larizza et al., 2012; Söllid and Thorsby, 1993). The newborns were followed by monthly stool sampling, periodic laboratory assays, and questionnaires regarding breastfeeding, diet, allergies, infections, family history, use of drugs, and clinical examinations. For this study, data from 74 infants per country were selected to be analyzed based on similar HLA risk class distribution and matching gender between the countries. The DIABIMMUNE study was conducted according to the guidelines laid down in the Declaration of Helsinki, and all procedures involving human subjects were approved by the local ethical committees of the participating hospitals. The parents and/or study subjects gave their written informed voluntary consent prior to sample collection.

Stool Sample Collection and DNA Extraction

Stool samples were collected by the participants' parents and stored in the household freezer (-20°C) until the next visit to the local study center; samples were then shipped on dry ice to the DIABIMMUNE Core Laboratory in Helsinki. The samples were then stored at -80°C until shipping to the Broad Institute for DNA extraction. DNA extractions from stool were carried out using the QIAamp DNA Stool Mini Kit (QIAGEN).

Library Construction, Sequencing, and Analysis of the 16S rRNA Gene and Shotgun Metagenomics

16S rRNA gene libraries were constructed as previously described by Kostic et al. (2015). Metagenomic libraries were prepared using Nextera XT DNA Library Preparation Kit (Illumina). 16S and metagenomic libraries were sequenced on the Illumina HiSeq 2500 platform. 16S data were processed using QIIME, and taxonomy was assigned according to Greengenes taxonomy map. Metagenomic data were analyzed using MetaPhlAn (v.2.2) (Truong et al., 2015) for taxonomic profiling and HUMAnN2 (<http://huttenhower.sph.harvard.edu/humann2>) for functional profiling. Associations with metadata were analyzed using MaAsLin, a linear modeling system adapted for microbial community data (<http://huttenhower.sph.harvard.edu/maaslin>). Metagenomic samples were additionally analyzed using ConStrains (Luo et al., 2015), which conducts within-species strain haplotyping by deconvoluting SNP patterns detected from mapping reads to species core genes across samples. See the [Supplemental Experimental Procedures](#) for detailed methodology.

Bacterial Strains and LPS Purification

The bacterial strains used in the study are summarized in Table S3. LPS purification was performed by hot phenol-water method (Hirschfeld et al., 2000).

Human Immune Stimulation Assays

Primary human PBMCs, in-vitro-differentiated monocyte-derived dendritic cells, or HEK293-NF- κ B reporter cells expressing hTLR4 were stimulated with the indicated doses of LPS purified from various strains (Table S3). In primary cells, cytokine concentrations in the supernatant after 24 hr were measured by cytokine bead array analysis (BD Biosciences). In HEK293 cells, stimulation was measured by Luciferase (BrightGlo, Promega).

Endotoxin Tolerance Assays

Primary monocytes were isolated from human PBMCs and incubated in the presence of LPS purified from *B. dorei* or *E. coli* at the indicated doses for 18–20 hr. Cells were then washed and cultured in cRPIMI for 3 days. Monocytes were challenged with a standard dose of 5 μ g/ml of zymosan. Supernatants were collected after 20 hr and analyzed using the cytokine bead array human inflammation kit (BD Biosciences) in accordance with the manufacturer's instructions.

Diabetes Incidence in NOD Mice

All animal studies were conducted under protocols approved by the Institutional Animal Care and Use Committee (IACUC) at NIBR. NOD/ShiLTj mice were purchased from Jackson Laboratory. Groups of 9 to 12 8-week-old mice were injected intraperitoneally with 10 μ g LPS purified from either *E. coli* or *B. dorei* once a week for 4 consecutive weeks. Non-fasting blood glucose was monitored weekly. The experimenter was blinded to the nature of the treatment for each group. Animals with either one reading above 300 mg/dl or two consecutive readings above 250 mg/dl were deemed diabetic.

Endotoxin Tolerance in NOD Mice

Groups of five mice were injected i.p. with 10 μ g LPS purified from either *E. coli* or *B. dorei*. After 24 hr, the splenocytes were isolated and restimulated in vitro with zymosan (2.5 μ g/ml). TNF α concentration was assessed by cytokine bead array after 24 hr.

ACCESSION NUMBERS

The accession number for the data reported in this paper has been uploaded to NCBI BioProject: PRJNA290380.

SUPPLEMENTAL INFORMATION

Supplemental Information includes Supplemental Experimental Procedures, seven figures, and three tables and can be found with this article online at <http://dx.doi.org/10.1016/j.cell.2016.04.007>.

AUTHOR CONTRIBUTIONS

T.V. and A.D.K. performed 16S and metagenomics data analysis. A.D.K. and T.D.A. performed qPCR to validate metagenomics data. E.H. and T.W.C. performed LPS purification and immunological assays and analyzed the data. T.V., A.D.K., E.H., T.W.C., E.A.F., H.V., C.H., D.G., and R.J.X. assembled and wrote the paper. T.V., A.D.K., E.H., T.W.C., V.T., S.M., D.G., M.K., and R.J.X. served as project leaders. H.S., A.-M.H., A.P., R.U., N.D., S.M.V., and M.K. designed the cohort study. A.D.K., E.H., T.W.C., J.A.P., and S.J.S. designed the LPS study. T.V., A.D.K., and D.G. designed the DNA sequencing experiments and sample management pipelines. T.V., E.A.F., M.Y., R.K., J.I., C.H., and D.G. led the method and research development. A.-M.H., A.P., V.T., R.U., S.M., N.D., J.I., and S.M.V. collected clinical samples. H.L., C.H., D.G., T.W.C., M.K., and R.J.X. served as principal investigators.

ACKNOWLEDGMENTS

We thank Tiffany Poon and Scott Steelman (Broad Institute) for help in sequence production and sample management, Leon Murphy (Novartis) for help with experimental design, Katriina Koski and Matti Koski (University of Helsinki) for the coordination and database work in the DIABIMMUNE study,

Chengwei Luo (Broad Institute) for help in the strain analysis, and Natalia Nedelsky (Massachusetts General Hospital) for editorial help in writing and figure generation. T.V. was supported by funding from JDRF and Hecse (Helsinki Doctoral Programme in Computer Science). H.L. and T.V. were supported by funding from the Academy of Finland Center of Excellence in Systems Immunology and Physiology Research. A.D.K received support as the Merck Fellow of the Helen Hay Whitney Foundation and as the Lawrence H. Summers Fellow of the Broad Institute. M.K. was supported by the European Union Seventh Framework Programme FP7/2007-2013 (202063) and the Academy of Finland Centre of Excellence in Molecular Systems Immunology and Physiology Research (250114). R.J.X. was supported by funding from JDRF, grants from the NIH (U54 DK102557, R01 DK092405, and P30 DK043351), funding from the Leona M. and Harry B. Helmsley Charitable Trust, and funding from the Center for Microbiome Informatics and Therapeutics at MIT.

Received: November 5, 2015

Revised: January 19, 2016

Accepted: March 31, 2016

Published: April 28, 2016

REFERENCES

- Abubucker, S., Segata, N., Goll, J., Schubert, A.M., Izard, J., Cantarel, B.L., Rodriguez-Mueller, B., Zucker, J., Thiagarajan, M., Henrissat, B., et al. (2012). Metabolic reconstruction for metagenomic data and its application to the human microbiome. *PLoS Comput. Biol.* 8, e1002358.
- Ardeshir, A., Narayan, N.R., Méndez-Lagares, G., Lu, D., Rauch, M., Huang, Y., Van Rompay, K.K., Lynch, S.V., and Hartigan-O'Connor, D.J. (2014). Breast-fed and bottle-fed infant rhesus macaques develop distinct gut microbiotas and immune systems. *Sci. Transl. Med.* 6, 252ra120.
- Aumeunier, A., Grela, F., Ramadan, A., Pham Van, L., Bardel, E., Gomez Alcalá, A., Jeannin, P., Akira, S., Bach, J.F., and Thieblemont, N. (2010). Systemic Toll-like receptor stimulation suppresses experimental allergic asthma and autoimmune diabetes in NOD mice. *PLoS ONE* 5, e11484.
- Bach, J.F. (2002). The effect of infections on susceptibility to autoimmune and allergic diseases. *N. Engl. J. Med.* 347, 911–920.
- Bach, J.F., and Chatenoud, L. (2012). The hygiene hypothesis: an explanation for the increased frequency of insulin-dependent diabetes. *Cold Spring Harb. Perspect. Med.* 2, a007799.
- Bäckhed, F., Roswall, J., Peng, Y., Feng, Q., Jia, H., Kovatcheva-Datchary, P., Li, Y., Xia, Y., Xie, H., Zhong, H., et al. (2015). Dynamics and stabilization of the human gut microbiome during the first year of life. *Cell Host Microbe* 17, 690–703.
- Biswas, S.K., and Lopez-Collazo, E. (2009). Endotoxin tolerance: new mechanisms, molecules and clinical significance. *Trends Immunol.* 30, 475–487.
- Cullen, T.W., Schofield, W.B., Barry, N.A., Putnam, E.E., Rundell, E.A., Trent, M.S., Degnan, P.H., Booth, C.J., Yu, H., and Goodman, A.L. (2015). Gut microbiota. Antimicrobial peptide resistance mediates resilience of prominent gut commensals during inflammation. *Science* 347, 170–175.
- Davis-Richardson, A.G., Ardissonne, A.N., Dias, R., Simell, V., Leonard, M.T., Kemppainen, K.M., Drew, J.C., Schatz, D., Atkinson, M.A., Kolaczkowski, B., et al. (2014). *Bacteroides dorei* dominates gut microbiome prior to autoimmunity in Finnish children at high risk for type 1 diabetes. *Front Microbiol* 5, 678.
- Gülden, E., Ihira, M., Ohashi, A., Reinbeck, A.L., Freudenberg, M.A., Kolb, H., and Burkart, V. (2013). Toll-like receptor 4 deficiency accelerates the development of insulin-deficient diabetes in non-obese diabetic mice. *PLoS ONE* 8, e75385.
- Hajjar, A.M., Ernst, R.K., Tsai, J.H., Wilson, C.B., and Miller, S.I. (2002). Human toll-like receptor 4 recognizes host-specific LPS modifications. *Nat. Immunol.* 3, 354–359.
- Herath, T.D., Wang, Y., Seneviratne, C.J., Lu, Q., Darveau, R.P., Wang, C.Y., and Jin, L. (2011). *Porphyromonas gingivalis* lipopolysaccharide lipid A

- heterogeneity differentially modulates the expression of IL-6 and IL-8 in human gingival fibroblasts. *J. Clin. Periodontol.* 38, 694–701.
- Hirschfeld, M., Ma, Y., Weis, J.H., Vogel, S.N., and Weis, J.J. (2000). Cutting edge: repurification of lipopolysaccharide eliminates signaling through both human and murine toll-like receptor 2. *J. Immunol.* 165, 618–622.
- Hofstad, T., Sveen, K., and Dahlén, G. (1977). Chemical composition, serological reactivity and endotoxicity of lipopolysaccharides extracted in different ways from *Bacteroides fragilis*, *Bacteroides melaninogenicus* and *Bacteroides oralis*. *Acta Pathol. Microbiol. Scand. [B]* 85, 262–270.
- Hunt, K.M., Foster, J.A., Forney, L.J., Schütte, U.M., Beck, D.L., Abdo, Z., Fox, L.K., Williams, J.E., McGuire, M.K., and McGuire, M.A. (2011). Characterization of the diversity and temporal stability of bacterial communities in human milk. *PLoS ONE* 6, e21313.
- Kallionpää, H., Laajala, E., Öling, V., Häkkinen, T., Tillmann, V., Dorshakova, N.V., Ilonen, J., Lähdesmäki, H., Knip, M., and Lahesmaa, R.; DIABIMMUNE Study Group (2014). Standard of hygiene and immune adaptation in newborn infants. *Clin. Immunol.* 155, 136–147.
- Kim, H.M., Park, B.S., Kim, J.I., Kim, S.E., Lee, J., Oh, S.C., Enkhbayar, P., Matsushima, N., Lee, H., Yoo, O.J., and Lee, J.O. (2007). Crystal structure of the TLR4-MD-2 complex with bound endotoxin antagonist Eritoran. *Cell* 130, 906–917.
- Koenig, J.E., Spor, A., Scalfone, N., Fricker, A.D., Stombaugh, J., Knight, R., Angenent, L.T., and Ley, R.E. (2011). Succession of microbial consortia in the developing infant gut microbiome. *Proc. Natl. Acad. Sci. USA* 108 (Suppl 1), 4578–4585.
- Kondrashova, A., Mustalahti, K., Kaukinen, K., Viskari, H., Volodicheva, V., Haapala, A.M., Ilonen, J., Knip, M., Mäki, M., and Hyöty, H.; Epivir Study Group (2008a). Lower economic status and inferior hygienic environment may protect against celiac disease. *Ann. Med.* 40, 223–231.
- Kondrashova, A., Viskari, H., Haapala, A.M., Seiskari, T., Kulmala, P., Ilonen, J., Knip, M., and Hyöty, H. (2008b). Serological evidence of thyroid autoimmunity among schoolchildren in two different socioeconomic environments. *J. Clin. Endocrinol. Metab.* 93, 729–734.
- Kostic, A.D., Gevers, D., Siljander, H., Vatanen, T., Hyötyläinen, T., Hämäläinen, A.M., Peet, A., Tillmann, V., Pöhö, P., Mattila, I., et al.; DIABIMMUNE Study Group (2015). The dynamics of the human infant gut microbiome in development and in progression toward type 1 diabetes. *Cell Host Microbe* 17, 260–273.
- Larizza, D., Calcaterra, V., Klersy, C., Badulli, C., Caramagna, C., Ricci, A., Brambilla, P., Salvaneschi, L., and Martinetti, M. (2012). Common immunogenetic profile in children with multiple autoimmune diseases: the signature of HLA-DQ pleiotropic genes. *Autoimmunity* 45, 470–475.
- Locascio, R.G., Niñonuevo, M.R., Kronewitter, S.R., Freeman, S.L., German, J.B., Lebrilla, C.B., and Mills, D.A. (2009). A versatile and scalable strategy for glycoprofiling bifidobacterial consumption of human milk oligosaccharides. *Microb. Biotechnol.* 2, 333–342.
- Luo, C., Knight, R., Siljander, H., Knip, M., Xavier, R.J., and Gevers, D. (2015). ConStrains identifies microbial strains in metagenomic datasets. *Nat. Biotechnol.* 33, 1045–1052.
- Marcobal, A., Barboza, M., Sonnenburg, E.D., Pudlo, N., Martens, E.C., Desai, P., Lebrilla, C.B., Weimer, B.C., Mills, D.A., German, J.B., and Sonnenburg, J.L. (2011). *Bacteroides* in the infant gut consume milk oligosaccharides via mucus-utilization pathways. *Cell Host Microbe* 10, 507–514.
- Markle, J.G., Frank, D.N., Mortin-Toth, S., Robertson, C.E., Feazel, L.M., Rolle-Kampczyk, U., von Bergen, M., McCoy, K.D., Macpherson, A.J., and Danska, J.S. (2013). Sex differences in the gut microbiome drive hormone-dependent regulation of autoimmunity. *Science* 339, 1084–1088.
- Morgan, X.C., Tickle, T.L., Sokol, H., Gevers, D., Devaney, K.L., Ward, D.V., Reyes, J.A., Shah, S.A., LeLeiko, N., Snapper, S.B., et al. (2012). Dysfunction of the intestinal microbiome in inflammatory bowel disease and treatment. *Genome Biol.* 13, R79.
- Needham, B.D., Carroll, S.M., Giles, D.K., Georgiou, G., Whiteley, M., and Trent, M.S. (2013). Modulating the innate immune response by combinatorial engineering of endotoxin. *Proc. Natl. Acad. Sci. USA* 110, 1464–1469.
- Peet, A., Kool, P., Ilonen, J., Knip, M., and Tillmann, V.; DIABIMMUNE Study Group (2012). Birth weight in newborn infants with different diabetes-associated HLA genotypes in three neighbouring countries: Finland, Estonia and Russian Karelia. *Diabetes Metab. Res. Rev.* 28, 455–461.
- Sai, P., and Rivereau, A.S. (1996). Prevention of diabetes in the nonobese diabetic mouse by oral immunological treatments. Comparative efficiency of human insulin and two bacterial antigens, lipopolysaccharide from *Escherichia coli* and glycoprotein extract from *Klebsiella pneumoniae*. *Diabetes Metab.* 22, 341–348.
- Seiskari, T., Kondrashova, A., Viskari, H., Kaila, M., Haapala, A.M., Aittoniemi, J., Virta, M., Hurme, M., Uibo, R., Knip, M., and Hyöty, H.; EPIVIR study group (2007). Allergic sensitization and microbial load—a comparison between Finland and Russian Karelia. *Clin. Exp. Immunol.* 148, 47–52.
- Sela, D.A., and Mills, D.A. (2010). Nursing our microbiota: molecular linkages between bifidobacteria and milk oligosaccharides. *Trends Microbiol.* 18, 298–307.
- Sela, D.A., Chapman, J., Adeuya, A., Kim, J.H., Chen, F., Whitehead, T.R., Lapidus, A., Rokhsar, D.S., Lebrilla, C.B., German, J.B., et al. (2008). The genome sequence of *Bifidobacterium longum* subsp. *infantis* reveals adaptations for milk utilization within the infant microbiome. *Proc. Natl. Acad. Sci. USA* 105, 18964–18969.
- Sokol, H., Pigneur, B., Watterlot, L., Lakhdari, O., Bermúdez-Humarán, L.G., Gratadoux, J.J., Blugeon, S., Bridonneau, C., Furet, J.P., Corthier, G., et al. (2008). *Faecalibacterium prausnitzii* is an anti-inflammatory commensal bacterium identified by gut microbiota analysis of Crohn disease patients. *Proc. Natl. Acad. Sci. USA* 105, 16731–16736.
- Solidi, L.M., and Thorsby, E. (1993). HLA susceptibility genes in celiac disease: genetic mapping and role in pathogenesis. *Gastroenterology* 105, 910–922.
- Stefka, A.T., Feehley, T., Tripathi, P., Qiu, J., McCoy, K., Mazmanian, S.K., Tjota, M.Y., Seo, G.Y., Cao, S., Theriault, B.R., et al. (2014). Commensal bacteria protect against food allergen sensitization. *Proc. Natl. Acad. Sci. USA* 111, 13145–13150.
- Teeäär, T., Liivak, N., Heilmann, K., Kool, P., Sor, R., Paal, M., Einberg, U., and Tillmann, V. (2010). Increasing incidence of childhood-onset type 1 diabetes mellitus among Estonian children in 1999–2006. Time trend analysis 1983–2006. *Pediatr. Diabetes* 11, 107–110.
- Truong, D.T., Franzosa, E.A., Tickle, T.L., Scholz, M., Weingart, G., Pasolli, E., Tett, A., Huttenhower, C., and Segata, N. (2015). MetaPhlAn2 for enhanced metagenomic taxonomic profiling. *Nat. Methods* 12, 902–903.
- von Mutius, E., and Vercelli, D. (2010). Farm living: effects on childhood asthma and allergy. *Nat. Rev. Immunol.* 10, 861–868.
- Voor, T., Julge, K., Bottcher, M.F., Jenmalm, M.C., Duchen, K., and Bjorksten, B. (2005). Atopic sensitization and atopic dermatitis in Estonian and Swedish infants. *Clin. Exp. Allergy* 35, 153–159.
- Watson, D.W., and Kim, Y.B. (1963). Modification of host responses to bacterial endotoxins. I. Specificity of pyrogenic tolerance and the role of hypersensitivity in pyrogenicity, lethality, and skin reactivity. *J. Exp. Med.* 118, 425–446.
- Wen, L., Ley, R.E., Volchkov, P.Y., Stranges, P.B., Avanesyan, L., Stober, A.C., Hu, C., Wong, F.S., Szot, G.L., Bluestone, J.A., et al. (2008). Innate immunity and intestinal microbiota in the development of type 1 diabetes. *Nature* 455, 1109–1113.
- Whitfield, C., and Trent, M.S. (2014). Biosynthesis and export of bacterial lipopolysaccharides. *Annu. Rev. Biochem.* 83, 99–128.

Supplemental Figures

Cell

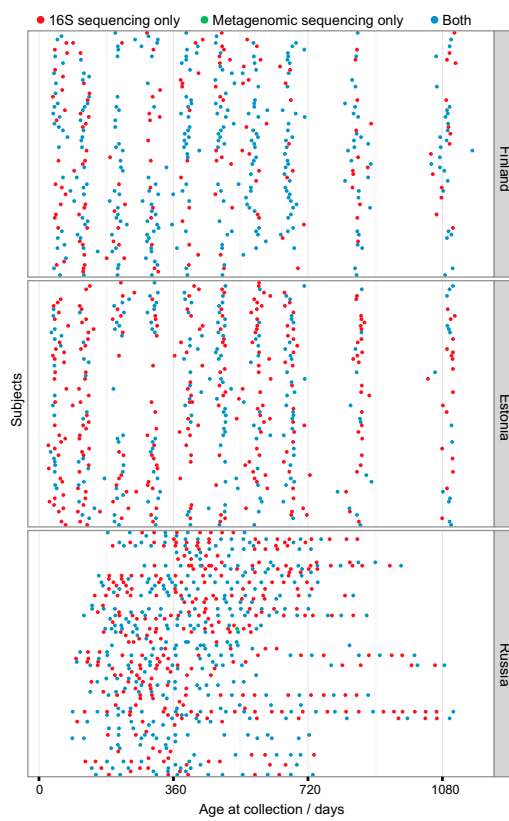


Figure S1. Sequencing Statistics, Related to Figure 1

Stool samples sequenced using 16S (red) or whole-genome shotgun sequencing (green); samples sequenced using both techniques are shown in blue. Rows in the panel represent subjects.

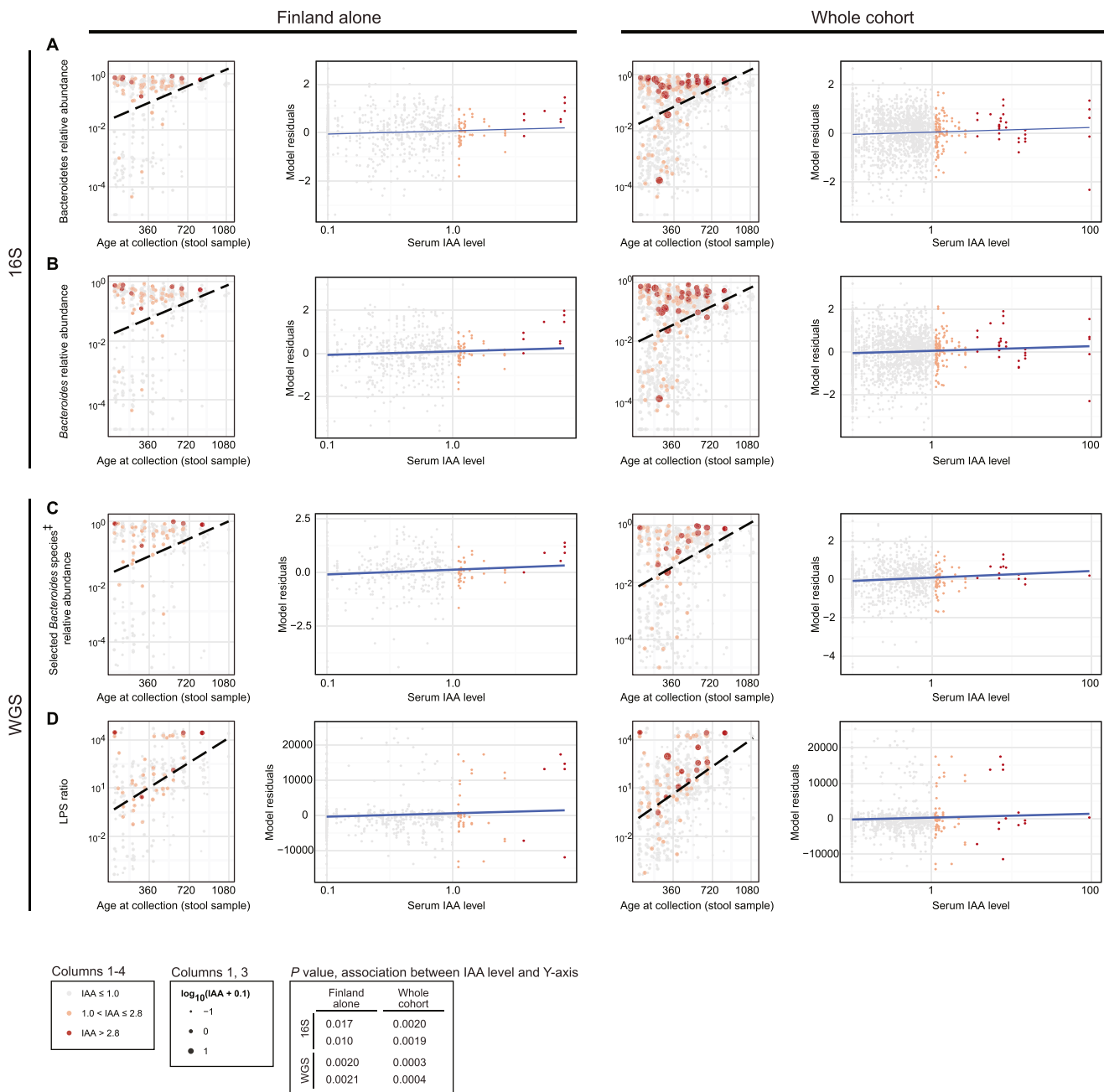


Figure S2. Correlations between Microbiome and Serum Insulin Autoantibody Levels, Related to Figure 2

(A–D) Each panel in this figure is comprised of four plots, one plot per column: first and third columns show how the correlations between IAA and microbial features are confounded by the age of stool sample collection within Finns and the whole cohort, respectively; measured microbial correlates on the y axis are plotted with respect to age at stool sample collection. Black dashed lines show the longitudinal trend (linear fit with respect to age); the size and color of the dots show the measured IAA levels for the corresponding serum sample (corresponding serum samples were collected 1–18 months after the stool sample). The significance of the correlation between IAA and microbial correlates was estimated using a mixed effect linear model with microbial correlate as a target variable, \log_{10} of IAA levels, age at collection (stool sample), and mode of delivery as fixed effects, and subject ID as a random effect. The following p values were obtained from the model. Second and fourth columns show the model residuals after effects of age, mode of delivery, and subject ID have been corrected from the data.

(A) Phylum Bacteroidetes (16S data): p = 0.017 (Finns), p = 0.0020 (all).

(B) Genus *Bacteroides* (16S data): p = 0.010 (Finns), p = 0.0019 (all).

(C) Combined relative abundance of *B. dorei*, *B. vulgatus*, *B. fragilis*, *B. stercoris*, *B. uniformis*, *B. ovatus*, *B. caccae*, *P. copri* (species with non-stimulatory LPS subtypes, WGS data): p = 0.0020 (Finns), p = 0.0003 (all).

(D) Estimate of the ratio between LPS derived from *Bacteroides* species in (C) and LPS derived from *E. coli* and *Klebsiella oxytoca* (WGS data): p = 0.0021 (Finns), p = 0.0004 (all).

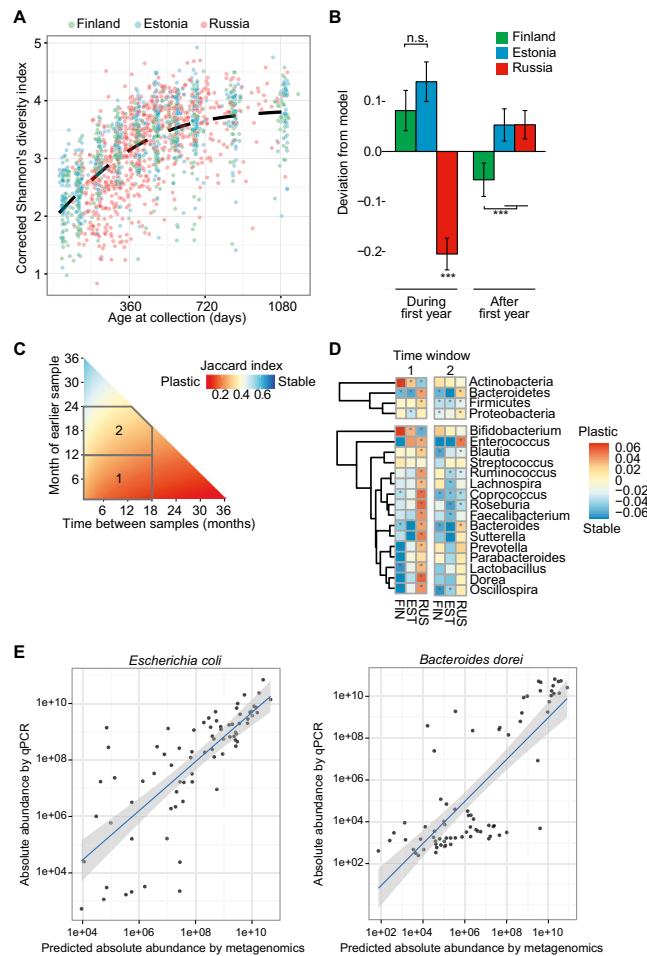


Figure S3. Gut Microbiome Diversity and Stability, Related to Figure 2

(A) Shannon's diversity index per sample estimated using 16S data and corrected for antibiotics and subject-specific random effects. Dashed line represents a sigmoid function fit.

(B) Comparison of residuals of the sigmoid function shown in (A). The residuals of the fit were compared using a Bayesian linear model by fitting a model with country as a factorial fixed effect, with the first-year samples and samples collected after the first year analyzed separately. Height of each bar represents the fixed effect coefficient per country; error bars show SD (68% credible intervals) of these coefficients. Positive numbers indicate higher diversity and negative numbers indicate lower diversity. n.s., not significant; *** $p < 0.001$, Bayesian linear model.

(C) Power law model used for modeling stability of the infant gut microbiota (see the [Supplemental Experimental Procedures](#)). The month of the earlier sample is shown on the vertical axis, and the time between the later and earlier sample is shown on the horizontal axis.

(D) An illustration of taxa-specific deviations from the power law fits given the model in (C). The heatmap shows the country-specific deviations from the model (i.e., more stable or plastic behavior in a given taxon) in two time windows (see C); asterisk denotes q -value < 0.01 (p values for the fixed effect terms given by a `bayesglm` model after correcting for multiple testing with Benjamini & Hochberg adjustment).

(E) Comparison between the absolute abundance measurements via qPCR and predictions of absolute abundances given the metagenomics data and total bacterial mass (estimated using universal 16S primers). Pearson correlation $r = 0.79$ for *B. dorei* and $r = 0.76$ for *E. coli*. x axis was computed by taking the product of relative abundance (given by the metagenomics data) and total bacterial load estimated using universal 16S primers. Both axes are on a log-scale.

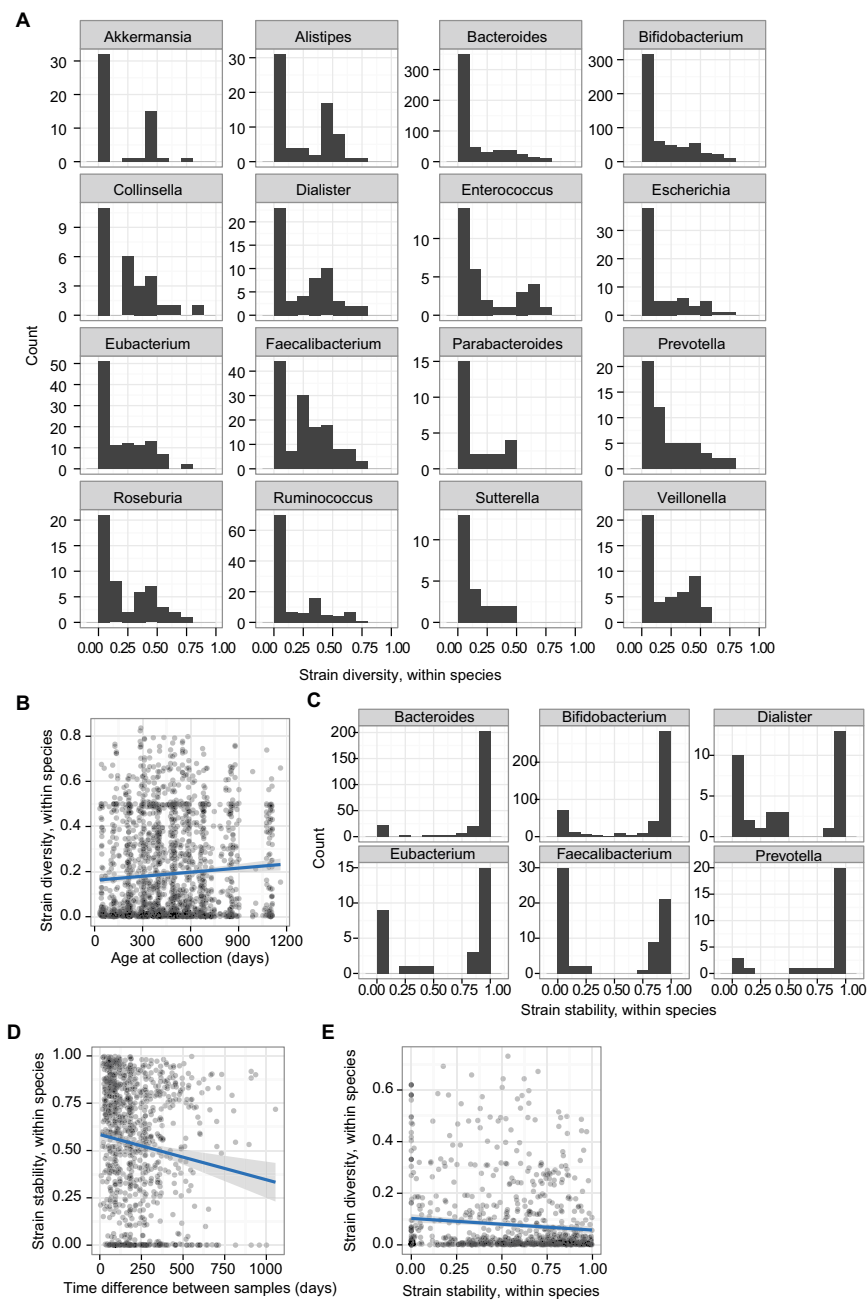
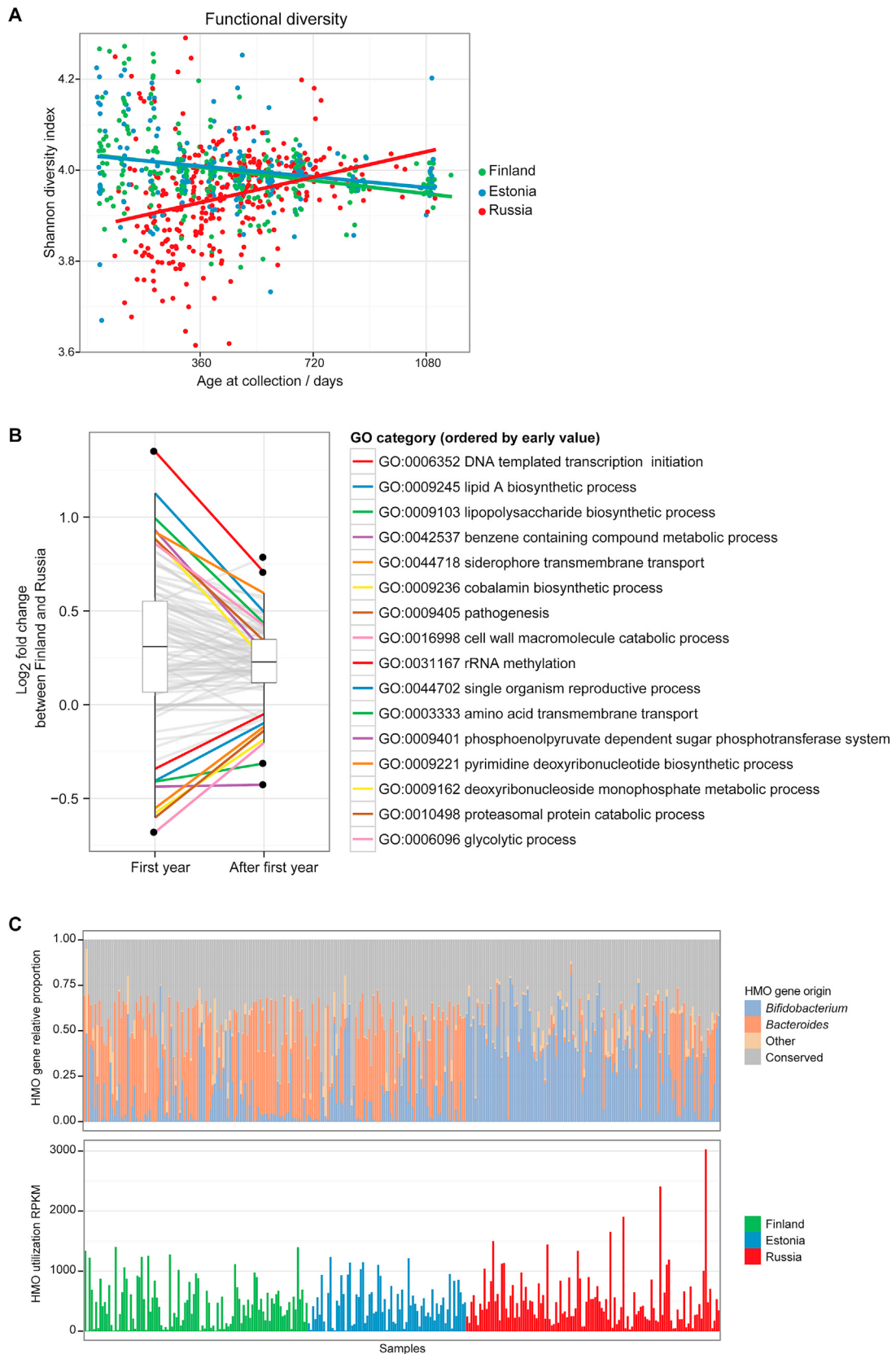


Figure S4. Gut Microbiome Diversity and Stability at the Strain Level, Related to Figure 2

- (A) The distributions of within-species strain diversity stratified by genera (shown for genera with more than 20 observations).
- (B) Observations of within-species strain diversity plotted against age of sample collection. Diversity is correlated with age, $r = 0.072$, $p = 8.6\text{e-}4$.
- (C) The distributions of within-species strain stability stratified by genera (shown for genera with more than 20 observations).
- (D) Observations of within-species strain stability plotted against the time difference between the compared samples. Stability is correlated with the time difference, $r = -0.124$, $p = 9.5\text{e-}5$.
- (E) Relationship between diversity and stability: within-species stability plotted against the mean of the within-species diversities of the two samples in the given stability observation. An inverse correlation was observed, $r = -0.107$, $p = 7.7\text{e-}4$.



(legend on next page)

Figure S5. Functional Potential of the Microbiota, Related to Figure 3

- (A) The diversity of functional potential of the microbiome per sample as measured by Shannon diversity of the distribution of GO categories.
- (B) GO categories that are differentially abundant between Finnish and Russian infants during the first year or after the first year. In the majority of categories, the difference is larger during the first year. Boxplots show median and interquartile range of the data.
- (C) Human milk oligosaccharide utilization gene abundance across the three countries within the first year of life, stratified by taxonomic origin of each gene. The samples are ordered by country (color in the bottom panel) and age of collection within countries (left = earliest samples), and both panels have same ordering. These data are averaged in [Figure 3B](#).

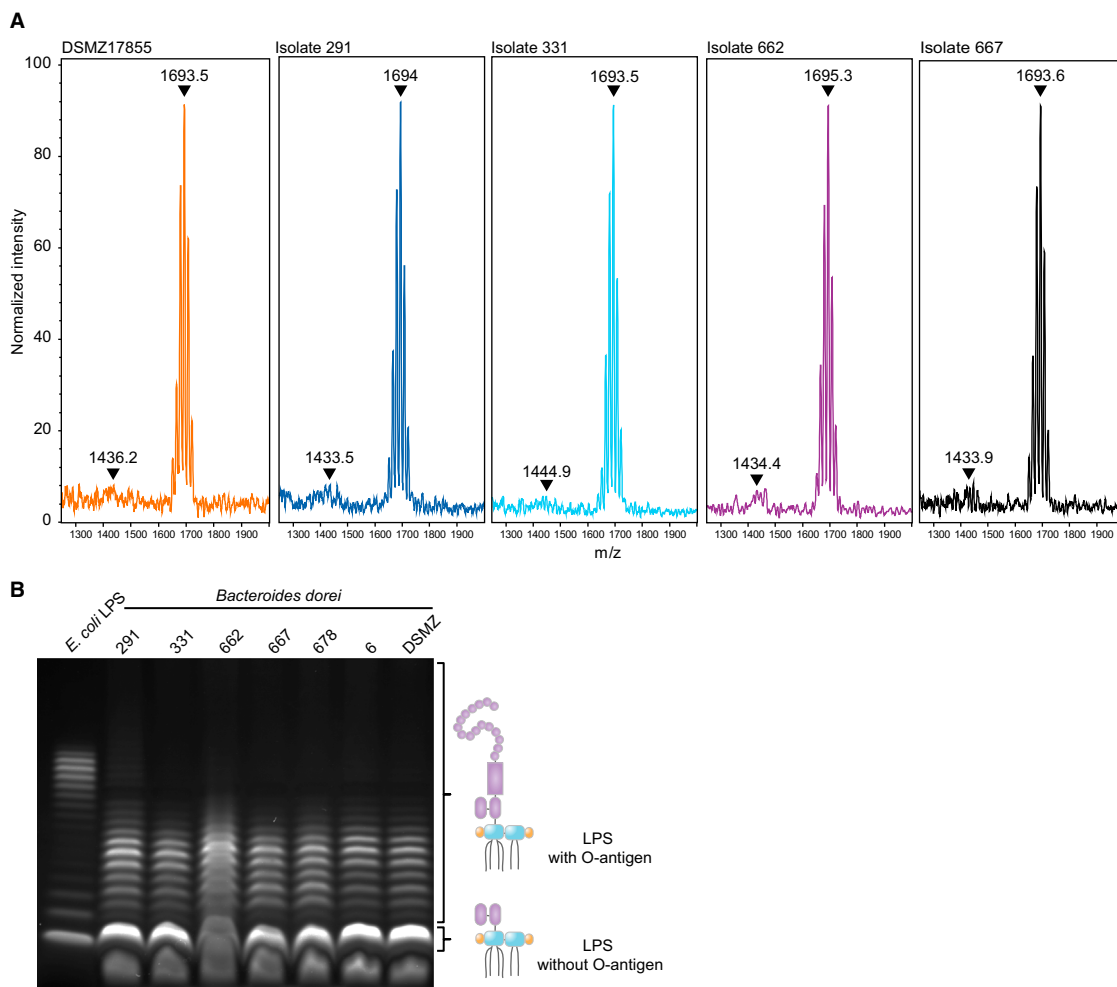


Figure S6. LPS Structural and Functional Features across *B. dorei* Isolates, Related to Figure 4

(A) MALDI-TOF MS analysis of lipid A purified from crude biomass of type strain (DSMZ) and four independent clinical isolates of *B. dorei*.

(B) SDS-PAGE gel stained with LPS-specific stain (Pro-Q Emerald) revealed a similar O-antigen staining pattern across 6 independent clinical isolates and the type strain of *B. dorei*. *E. coli* LPS was used as a positive staining control.

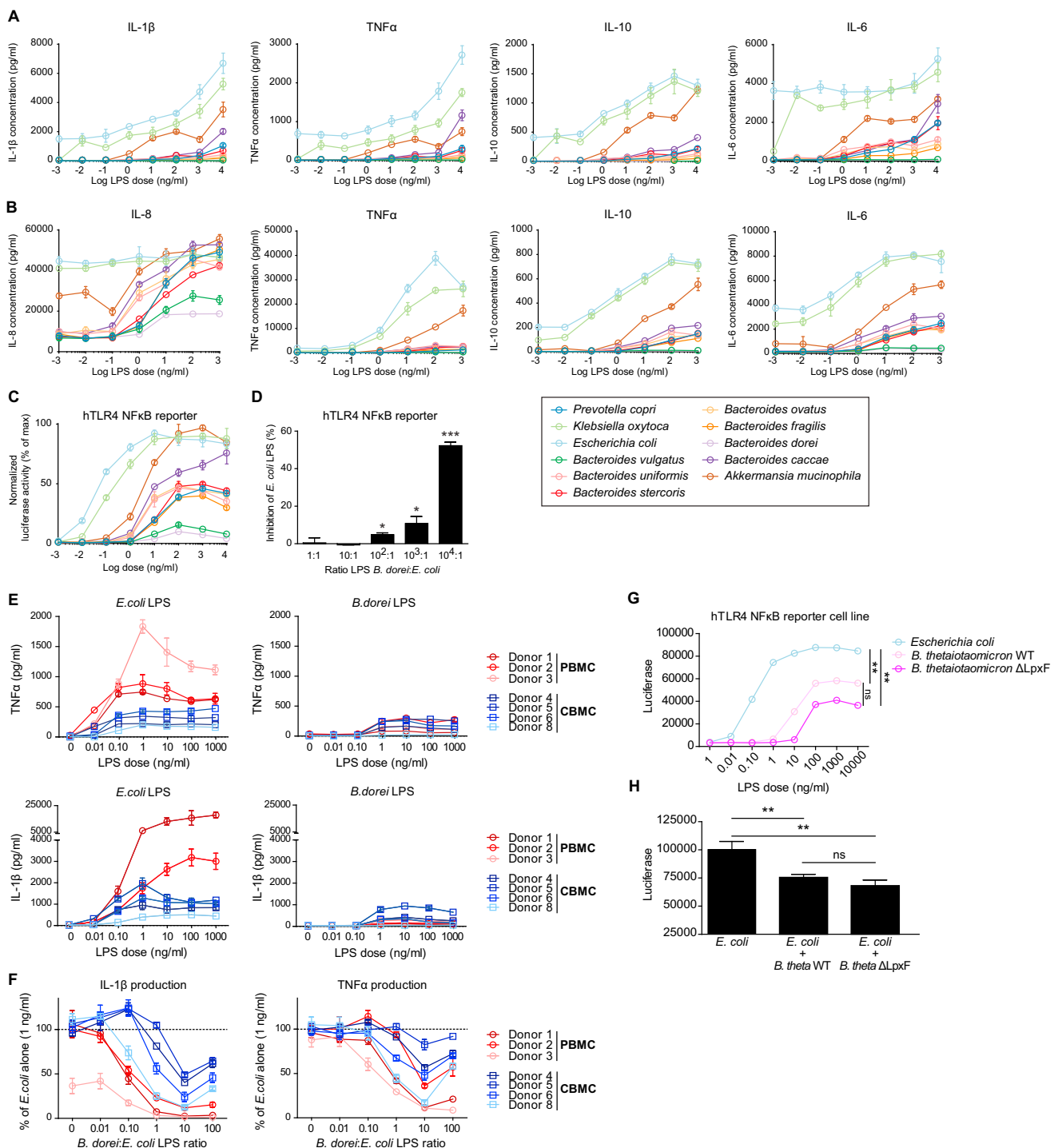


Figure S7. Stimulation of Primary Immune Cells and TLR4 Reporter Cells by LPS from Different Bacterial Strains, Related to Figure 5

LPS isolated from individual bacterial strains was used to stimulate human PBMCs, human monocyte-derived dendritic cells, or HEK293 NF κ B-luciferase reporter cells expressing human TLR4.

(A and B) Human PBMCs (A) or monocyte-derived dendritic cells (B) were stimulated for 16–18 hr with LPS from indicated bacterial strains, after which supernatants were collected and analyzed by cytokine bead array. Results are expressed as mean concentration and SD of triplicate assessments. Data are representative of three independent experiments.

(C) Reporter cells expressing human TLR4 were stimulated with LPS from indicated bacterial strains for 6 hr and NF κ B activity was measured by luciferase activity. Activity is expressed as percent of maximum luciferase signal. Data are represented as mean and SD of triplicate assessments.

(legend continued on next page)

- (D) Inhibition by *B. dorei* LPS of NF κ B activation by 1 ng/ml *E. coli* LPS in hTLR4 reporter cells. Data are represented as mean and SD of triplicate assessments.
*p < 0.05, **p < 0.0005 by Student's t test compared to *E. coli* stimulation.
- (E) Human primary PBMCs (3 donors) and CBMCs (4 donors) were stimulated in the presence of increasing doses of *E. coli*- or *B. dorei*-derived LPS. Supernatants were collected after 24 hr of culture, and TNF α (upper) and IL1 β (middle) concentrations were assessed by CBA. Data are shown as mean and SD of triplicate assessments.
- (F) PBMCs and CBMCs were stimulated with 1 ng/ml *E. coli* LPS and increasing doses of *B. dorei* LPS. Supernatants were collected at 24 hr, and TNF α and IL1 β concentrations were assessed by CBA. Data are shown as mean and SD of triplicate assessments. All donors were Caucasians. Cells were procured as frozen isolated mononuclear cells from commercial vendors.
- (G) HEK293 NF κ B-reporter cells expressing hTLR4, hMD2, and hCD14 were stimulated with increasing doses of LPS isolated from *B. thetaiotaomicron* WT (1'-mono-phosphorylated) or lacking LpxF (1,4-bis-phosphorylated). Luciferase activity was measured after 6 hr.
- (H) hTLR4-expressing NF κ B reporter cells were stimulated with *E. coli* LPS alone or in combination with LPS from the indicated organisms. Luciferase activity was measured after 6 hr. Data are represented as mean and SD of triplicate assessments. (Note: *Bacteroides* spp. = both *B. thetaiotaomicron* and *B. dorei*.)
**p < 0.005, n.s., not significant, ANOVA with Holm-Sidak multiple comparison post-test for panels G and H.

Supplemental Information

Variation in Microbiome LPS Immunogenicity

Contributes to Autoimmunity in Humans

Tommi Vatanen, Aleksandar D. Kostic, Eva d'Hennezel, Heli Siljander, Eric A. Franzosa, Moran Yassour, Raivo Kolde, Hera Vlamakis, Timothy D. Arthur, Anu-Maaria Hämäläinen, Aleksandr Peet, Vallo Tillmann, Raivo Uibo, Sergei Mokurov, Natalya Dorshakova, Jorma Ilonen, Suvi M. Virtanen, Susanne J. Szabo, Jeffrey A. Porter, Harri Lähdesmäki, Curtis Huttenhower, Dirk Gevers, Thomas W. Cullen, Mikael Knip, Ramnik J. Xavier, and DIABIMMUNE Study Group

Supplemental Experimental Procedures

Study Cohort

832 newborns were recruited to the birth cohort as part of the international DIABIMMUNE study (<http://www.diabimmune.org/>), for which the consent rate was 80% in Tartu, Estonia, 59% in Espoo, Finland, and 24% in Petrozavodsk, Russia. Recruitment took place between September 2008 and May 2010 in Estonia and Finland, and between September 2008 and July 2011 in Russia. Follow-up was completed in April 2013 in Estonia and Finland, and in October 2013 in Russia. The final number of children included in the present study was 74 from each country. This cohort does not have overlapping subjects with another DIABIMMUNE microbiome cohort studied in Kostic et al. (Kostic et al., 2015). Inclusion criteria included positive cord blood testing for HLA DR-DQ alleles conferring increased risk for autoimmunity. The participating children were monitored prospectively for infections, use of drugs including antibiotics, and other life events. Data on breastfeeding and introduction of complementary foods were registered in a study booklet and interview at each study visit (3, 6, 12, 18, 24, and 36 months). Serum samples were collected from all infants during visits to the clinic at the following time points: 0 (cord blood), 3, 6, 12, 18, 24, and 36 months. Diabetes-associated autoantibodies were analyzed as previously described (Kostic et al., 2015). Celiac disease seropositivity was measured by anti-transglutaminase IgA levels using a fluoroenzyme immunoassay (ImmunoCAP EliA Celkey system; ThermoFisher Scientific, Uppsala, Sweden). Subject metadata is available in Table S1. The DIABIMMUNE study was conducted according to the guidelines laid down in the Declaration of Helsinki, and all procedures involving human subjects were approved by the local ethical committees of the participating hospitals. The parents and/or study subjects gave their written informed voluntary consent prior to sample collection.

Metagenome Library Construction

Whole-genome shotgun sequencing libraries were prepared as follows. Metagenomic DNA samples were quantified by Quant-iT PicoGreen dsDNA Assay (Life Technologies) and normalized to a concentration of 50 pg/ μ L. Illumina sequencing libraries were prepared from 100–250 pg DNA using the Nextera XT DNA Library Preparation kit (Illumina) according to the manufacturer's recommended protocol, with reaction volumes scaled accordingly. Batches of 24, 48, or 96 libraries were pooled by transferring equal volumes of each library using a Labcyte Echo 550 liquid handler. Insert sizes and concentrations for each pooled library were determined using an Agilent Bioanalyzer DNA 1000 kit (Agilent Technologies).

Sequencing and Analysis of the 16S Gene and Whole-Genome Shotgun Metagenomics

16S sequencing was performed essentially as previously described (Gevers et al., 2014). Because the Russians had a lower level of compliance (28% for stool sample collection), we sequenced all available Russian samples and used sparse sampling of the available Finnish and Estonian samples to achieve equal sample numbers (Figure S1). Taxonomy was assigned using the Greengenes predefined taxonomy map of reference sequence OTUs to taxonomy (McDonald et al., 2012). The resulting OTU tables were checked for mislabeling (Knights et al., 2011b) and contamination (Knights et al., 2011a). A mean sequence depth of 57,110 per sample was obtained, and samples with fewer than 3,000 filtered sequences were excluded from analysis.

Samples for whole-genome shotgun metagenomics sequencing were selected by first including the more densely sampled subjects (242 samples from 12 Finnish and 15 Russian subjects, with 7 samples or more per subject), and complemented by a set of the 543 samples using “representative sampling” (see below) on the basis of 16S data using microPITA (Tickle et al., 2013), resulting in a dataset of 785 metagenomics samples from 214 infants. The term “representative sampling” refers to an unsupervised manner of selecting WGS samples such that they evenly capture the microbial variability of all samples. Technically, this involves tiling the “space” of all samples with representatives roughly equidistant from their non-selected neighbors. More information about microPITA and representative sampling is given at <https://huttenhower.sph.harvard.edu/micropita>.

Principal coordinate plots

Principal coordinate plots were generated using t-Distributed Stochastic Neighbor Embedding (t-SNE) as implemented in the R package Rtsne. Bray-Curtis dissimilarity, $BC_{ij} = \sum_s |x_{si} - x_{sj}| / \sum_s |x_{si} + x_{sj}|$, where x_{si} denotes the abundance of strain s in sample i , was used as the distance measure. We followed the guidelines given by the authors (FAQ at <http://lvdmaaten.github.io/tsne/>) and selected the free parameter, perplexity, by generating mappings with perplexity values between 5 and 50 in increments of 5. Mappings with lowest error and best visual properties were obtained using perplexity = 50, which is the value used in Figure 2A.

Diversity Analysis Based on 16S Data

Microbial diversity (alpha diversity) was measured using Shannon's diversity index, $H = -\sum p_i \log_2 p_i$, on OTU-level data. To account for the decrease in diversity caused by antibiotics exposure and subject-level random effects, the data were first corrected for these confounders using a linear mixed effects model (MEM); Figure S3A shows the corrected alpha diversities obtained using the model residuals for a MEM with antibiotics exposure as a fixed effect and subject IDs as random effect (antibiotics exposure was represented as a binary indicator of whether a sample was collected within one month of antibiotics exposure). To account for age-dependent effects and non-uniform sampling between countries, a sigmoid function $y = a/(1 + e^{-bx+c})$ was fitted using the residual data (*nls* function in R). This model provided the best fit to our data (as measured by the Bayesian information criterion) in comparison with other candidate models (linear, log-linear, Hill function, and hyperbolic tangent function). The residuals of this fit were then compared using a Bayesian linear model (*bayesglm* function of *arm* package in R) by fitting a model with country as a factorial fixed effect for the first-year samples and samples collected after the first year separately. Figure S3B shows fixed-effect coefficients of these models (bars) as well as their standard deviations (error bars).

Stability Analysis Based on 16S Data

The Jaccard index for a given sample pair is defined as $|sample A \cap sample B| / |sample A \cup sample B|$, i.e., the number of items (here, OTUs) in common between samples A and B divided by the total number of items present in either sample A or sample B. The Jaccard index was calculated for all within-subject sample pairs and further stratified by taxa, requiring > 10 OTUs per taxonomic group for a taxon to be included in the analysis. Jaccard indices were modeled using a power law adapted from Faith et al., (Faith et al., 2013), $Jaccard\ index = a \cdot t_{diff}^b + c \cdot t_{earlier}$, where t_{diff} is the time between the collection of the samples and $t_{earlier}$ is the collection time of the earlier of the samples (*nls* function in R). Figure S3C shows the model for all OTUs (not stratified by taxa).

For each modeled phylum and genus, model residuals were calculated from the model described above. Residuals per taxon were then compared using a Bayesian linear model (*bayesglm* function of *arm* package in R) by fitting a model with country as a factorial fixed effect for residuals in two time windows shown in Figure S3C.

Log₂ fold changes between Finland and Russia

Log₂ fold changes between Finland and Russia in different taxonomic groups in Figure 2D were computed as follows: for each taxon, relative abundance data were bootstrapped 1,000 times and the log₂ ratio of the medians of relative abundances per country was computed for each bootstrap dataset. Species-level log ratios with a bootstrapped zero median were adjusted with a pseudoabundance of 10⁻⁵ to avoid zero division when necessary. Bars in Figure 2D show mean bootstrap estimates (mean of all computed fold changes) and error bars show SD of bootstrap estimates for each taxon. Statistical significances and number of samples per comparison are shown in online results at <http://pubs.broadinstitute.org/diabimmune>.

Average Microbial Composition

Country-level average microbial profiles were generated using the following sliding window averaging analysis. For the phylum-level plot in Figure 2C, phyla with mean relative abundance less than 0.01 (1%) were removed from the analysis. Average phylum composition was computed in a sliding window of size 90 days, with step size of 10 days. At least 15 samples were required to include the average profile in the plot, hence early averages are missing from Russian plots in Figure 2C. In Figure 2C, $n = 448$ for Finns, $n = 472$ for Estonians, and $n = 664$ for Russians. For the species-level plot in Figure 3D, average relative abundances were computed for the species of interest (the top 15 species contributing to the LPS signal) as described above using a sliding window of size 180 days. In Figure 3D, $n = 283$ for Finns, $n = 199$ for Estonians, and $n = 303$ for Russians.

Calling Differentially Abundant Taxa and Species

Associations between clinical metadata and taxon abundances were tested using *MaAsLin*, a linear modeling system adapted for microbial community data (<http://huttenhower.sph.harvard.edu/maaslin>; default parameters were used). In brief, *MaAsLin* applies a generalized linear model using each clade as an independent response variable after outlier removal (Grubbs test), a variance stabilizing arcsin square root transform for binomial data, dimensionality reduction by boosting, and false discovery rate multiple hypothesis correction (Morgan et al., 2012). The analysis

was conducted separately for (1) all samples, (2) samples collected during the first year of life, (3) samples collected after the first year of life. Furthermore, allergy and IgE measurements were available for only a subset of subjects and were tested using a separate model with fewer samples. Twenty-eight Russian subjects with no diet or breastfeeding information were excluded from the analysis (Table S1). Results tables and scripts for replicating all analyses can be found online at <http://pubs.broadinstitute.org/diabimmune>.

The following binary dietary variables indicating whether the given dietary compound had been introduced (or in case of breastfeeding, whether it was still ongoing) were used as fixed effects in all models: breastfeeding, infant formula, rice, wheat, oats, barley, cereal, root vegetables, vegetable, eggs, soy, milk, and meat. In addition, we included the following dietary variables in all but the first-year models (the given compounds were not yet introduced during the first year): fresh fruits, corn, and fish. The following binary variables were used in all models: gender, mode of delivery (caesarean section versus vaginal delivery), antibiotics use within one month of sample collection, and seroconversion status (T1D autoantibody positivity). The following factorial variables were used in all models: country and HLA risk class. The following continuous variables were used as fixed effects in all models: age at collection in days, length of breastfeeding in months, number of preceding antibiotics prescriptions, and sample sequence depth. The following variables were used as random effects in all models: subject ID and sequencing batch ID (16S or whole-genome shotgun). The following variables were included in models using a subset of subjects with available clinical metadata: \log_{10} of total IgE in serum measured during the second year of life, a binary variable indicating a high total IgE measurement, and binary variables indicating allergic sensitization to milk, egg, peanuts, dust mites, cat dander, dog dander, birch, and timothy.

Random Forest Classification

Random forests (RFs) were trained using samples in time windows between 170 and 260 days, $n = 40/38/102$ (FIN/EST/RUS); based on 16S data on genus level using the R package *randomForest*. For each pairwise classification task, a Random forest with 25,000 trees was trained. The ROC curves were generated using the R package *ROCR* using the out-of-bag predictions for classification. Within the three-month window, age of collection per sample was not controlled for. As each infant's microbiome will develop at an individual pace, stratifying by age within a smaller time window would not be likely to further improve the Random Forest analysis.

Analysis of Metagenomics Samples

Metagenomic libraries were sequenced on the Illumina HiSeq 2500 platform, targeting ~2.5 Gb of sequence per sample with 101 bp, paired-end reads. Reads were quality controlled by trimming low-quality bases, dropping reads below 60 nucleotides, and filtering out potential human contamination; these steps were performed using the *KneadData* pipeline (<https://bitbucket.org/biobakery/kneaddata>). Quality controlled samples were profiled taxonomically using MetaPhlAn 2.0 (Truong et al., 2015), following Bowtie 2-2.1.0 (Langmead and Salzberg, 2012) alignment to the MetaPhlAn 2.0 unique marker database (<http://huttenhower.sph.harvard.edu/metaphlan2>). Samples were profiled functionally using HUMAnN2 (<http://huttenhower.sph.harvard.edu/humann2>) (Abubucker et al., 2012). Briefly, HUMAnN2 maps metagenomic reads to the pangenomes (Huang et al., 2014) of species identified upstream in the taxonomic profiling step. Protein-coding sequences in these pangenomes have been pre-annotated to their respective UniRef50 families (Supek et al., 2015), which serve as a comprehensive, non-redundant protein sequence database. Reads that do not align to a known pangome are separately mapped to the entirety of UniRef50 by translated search with DIAMOND (Buchfink et al., 2015). All hits are weighted based on alignment quality and sequence length, with per-species and unclassified hits combined to produce community totals for each protein family (in addition to species-stratified totals) in RPK (reads per kilobase) units. RPK units were further normalized to RPKM units (reads per kilobase per million sample reads) to account for variation in sequence depth across samples.

Interpolation of Absolute Abundance by Quantitative PCR

Quantitative PCR (qPCR) was performed to interpolate the absolute abundance of *B. dorei* and *E. coli* species in DNA from 85 subject stool samples that we had archived from this study using previously described methods (Nakatsuji et al., 2013). Primer sequences for qPCR for these species were obtained from the literature (Lee et al., 2010; Odamaki et al., 2008). Primers were tested against the following strains to test for specificity: *Bacteroides fragilis*, *Bacteroides thetaiotaomicron*, *Bacteroides vulgatus*, *Bacteroides caccae*, and *Parabacteroides distasonis* to test for *B. dorei* specificity, and *Klebsiella oxytoca* to test for *E. coli* specificity. The primers did not show cross-reactivity to any of these species. To interpolate approximate colony-forming units (CFU) per gram of stool from the

DNA, a standard curve was created by growing 10-fold serial dilutions of a type strain from each species and regressing the Ct value from the qPCR of each dilution against the CFU from each dilution. The CFU/g stool for *B. dorei* and *E. coli* was obtained by interpolating the qPCR Ct value from this standard curve and normalizing for the mass of stool that was used for the DNA purification. Total bacterial load was determined by qPCR using universal bacterial 16S primers (Atarashi et al., 2011). Predictions of absolute abundances given the metagenomics data were computed by multiplying the total bacterial mass with relative abundance predicted by the metagenomics data. In Figure S3E, pseudocount 1e-5 was added to relative abundances predicted by metagenomics data to account for limitations in metagenomics to detect very lowly abundant bacterial species.

Strain Haplotyping Using ConStrains

ConStrains (Luo et al., 2015) (<https://bitbucket.org/luo-chengwei/constrains>) conducts within-species strain haplotyping by deconvoluting SNP patterns detected from mapping reads to species pangenomes across samples. Samples were processed by including all samples from a given subject in the same analysis, allowing us to follow within-subject strain profile evolution in time and compute strain stability (see below). ConStrains requires 10x coverage of a given pan genome to reliably identify strains within its corresponding species. As a result, a larger number of strain profiles could be constructed for species that tended to occur with higher metagenomic abundance (Figures S4A and S4C).

From the obtained strain-level abundance profiles, we computed species- and sample-specific haplotype diversity scores, $H = 1 - \sum p_i^2$, where p_i denotes the abundance of strain i . This measure was motivated by the concept of heterozygosity in population genetics, and is bounded between [0,1]. A convenient probabilistic interpretation follows: given two randomly sampled bacterial cells from species X in sample Y, the corresponding haplotype diversity score reflects the probability that the two cells derive from different strains. We measured strain-level stability using Bray-Curtis dissimilarity, $BC_{ij} = \sum_s |x_{si} - x_{sj}| / \sum_s |x_{si} + x_{sj}|$, where x_{si} denotes the abundance of strain s in sample i . All within-subject pairwise comparisons for samples with strain calling results were included in the stability analysis.

GO Functional Annotation

Functional profiling of the metagenomes yielded abundance measurements for tens of thousands of microbial gene families. To make downstream analysis of these families more tractable, we grouped gene family abundance into broader functional categories based on annotations between UniProt proteins (UniProt, 2015) (of which our ~11 million UniRef50 protein families are a subset) and gene ontology (GO) (Dimmer et al., 2012; Gene Ontology, 2015). We focused on the “Biological Process” hierarchy within GO, allowing protein annotations to propagate upward through the child-parent relationships among GO terms. For example, a protein annotated with the term “carbohydrate metabolism” was automatically annotated to that term’s less specific parent, “primary metabolic process.” Following previous work (Huang et al., 2007; Zhou et al., 2002), we isolated a subset of “informative” GO terms, defined as terms associated with $>k$ proteins for which no descendant term was associated with $>k$ proteins (here, $k = 2,000$, which equates to ~1 of every 5,000 UniRef50 protein families). This procedure yielded a comprehensive but manageable set of 247 non-redundant GO Biological Process terms for subsequent analysis. By the nature of their construction, informative GO terms tend to provide more resolution for well-conserved and well-studied processes (which are annotated to many proteins) and place less focus on highly specific processes associated with only a small number of proteins.

Testing Differently Abundant GO Categories

Abundances of the resulting categories were compared between Finnish and Russian children by the following procedure: (1) pseudocount 2⁷ was added to RPKM data in order to stabilize the variation in lowly abundant categories; (2) log₂-transformed data were modeled using a mixed effect model (*glmmPQL* from the *MASS* package in R) with subject ID, mode of delivery, and breastfeeding status as random effects and “age at collection” and country (Finland versus Russia) as fixed effects; (3) the nominal p-values for the country fixed effect coefficient were adjusted using the Benjamini-Hochberg method; (4) categories with corrected $p < 0.1$ were considered statistically significant. Data on all categories discussed in this paper were checked using Shapiro-Wilk test for normality and F test for equal variance between groups.

Human milk oligosaccharide gene cluster analysis

To determine which bacteria, if any, contribute to HMO utilization in each country, the entire HUMAnN2 ChocoPhlAn database (a collection of pangomes assembled from NCBI reference genomes, see Supplemental Experimental Procedures) was aligned against a fully annotated HMO gene cluster (Sela et al., 2008) to obtain a collection of HMO utilization genes. This gene family-HMO utilization gene mapping (stratified by species) allowed the quantification of HMO utilization per sample, and further stratification by contributing genera. Genes that did not belong to a *Bifidobacterium* or *Bacteroides* species were labeled as “Other.” Genes that were too highly conserved to confidently assign to a unique genus were labeled as “Conserved.”

Correlations between Microbiome and Serum IAA

We assessed associations between serum insulin autoantibody (IAA) levels and microbiome by pairing each serum sample with stool samples collected more than one month and less than 19 months before the serum collection time point. This analysis was designed to measure whether properties of the microbiome correlated with IAA measurements. All correlations were tested using a linear mixed effect models where the properties of microbiome were used as target variable and \log_{10} of IAA levels, age of collection, and mode of delivery were used as fixed effect predictors. Additionally, we used a fixed effect term for country when applicable (i.e., comparison in the whole cohort), and subject ID as a random effect.

Using the 16S data, phylum Bacteroidetes and genus *Bacteroides* correlated with serum IAA levels (Figures S2A and S2B), both within Finland and cohort-wide. Combined relative abundance of *B. dorei*, *Bacteroides vulgatus*, *Bacteroides fragilis*, *Bacteroides stercoris*, *Bacteroides uniformis*, *Bacteroides ovatus*, *Bacteroides caccae*, and *P. copri* -- species that were found to have the least immunostimulatory LPS subtypes -- also correlated with IAA levels (Figure S2C). The correlation is more significant across the whole cohort (compared to Finns alone), implying that the trend in Russia and Estonia is in concordance with Finns even though the association is not statistically significant when analyzing data from these countries alone.

Finally, we examined the predicted ratio between non-immunogenic LPS (i.e., derived from *Bacteroides* species above and *P. copri*) and immunostimulatory LPS (i.e., derived from *E. coli* and *Klebsiella oxytoca*), finding that the LPS ratio correlated with serum IAA levels (Figure S2D). The median ratio was 20-fold higher in Finns compared to Russians; the median ratio was 5:1 in Finns as compared to 1:4 in Russians. The LPS abundances were estimated using WGS data by using GO category lipid A biosynthesis RPKM as a proxy for LPS quantity. The LPS ratio was greater than 10:1 in 12 of 14 data points (8 separate subjects, two dots are overlapping) where IAA value was greater than 2.8 (seroconversion threshold).

Bacterial Strains and Growth Conditions

The bacterial strains used in the study are summarized in Table S3. *Bacteroides thetaiotaomicron* strains (WT and $\Delta LpxF$) have been previously described (Cullen et al., 2015). All strains were started from 20% glycerol stocks stored at -80°C, plated onto brain heart infusion (BHI) agar supplemented with hemin and vitamin K (Teknova; B1093), and grown anaerobically at 37°C. Liquid cultures of all strains were started from a single colony inoculated into 1000 ml BHI liquid media supplemented with 10 ml vitamin K-hemin solution (BD; 212354), 10 ml trace minerals (ATCC; MD-TMS), 10 ml trace vitamins (ATCC; MD-VS), 50 ml fetal bovine serum (Hyclone; SH30071), and grown anaerobically at 37°C. A flexible anaerobic chamber (Coy Laboratory Products) containing 20% CO₂, 10% H₂, and 70% N₂ was used for all anaerobic microbiology steps.

Lipopolysaccharide Purification and Analysis

LPS from all strains were isolated from a 1000-ml liquid culture grown under standard conditions for ~48 h using the hot water-phenol method as previously described. To remove trace amounts of endotoxin protein, phenol-purified LPS was further treated as described (Hirschfeld et al., 2000), with the modifications described below. Following the final ethanol precipitation, LPS was lyophilized to determine the yield using a Mettler Toledo XS105 Dual Range analytical balance (sensitivity ≥ 0.1 ng), and resuspended in HyPure cell culture-grade endotoxin-free water (Hyclone) to a final concentration of 1 mg/ml without the addition of triethanolamine. Lipopolysaccharides were analyzed using the Pro-Q Emerald 488 in-gel staining kit (Thermo Fisher Scientific) according to the manufacturer’s instructions.

Isolation of Lipid A for Mass Spectrometry Analysis

For analysis of crude biomass, pellets from 10 ml overnight broth bacterial cultures were washed 3 times in water, methanol and chloroform (0.8:1:2). Alternatively, purified LPS (200 μ g) was used directly. The material was

subjected to mild acid hydrolysis at 100°C for 30 minutes in 12.5 mM sodium acetate buffer, pH 4.5, in the presence of 1% SDS to break the Kdo linkage and free lipid A was recovered by two-phase Bligh/Dyer extraction (Zhou et al., 1999; Zhou et al., 1998). The lipid A species were analyzed using a matrix-assisted laser desorption/ionization time of flight mass spectrometer (BRUKER, Ultraflex) equipped with a smartbeam laser using a 2-kHz firing rate. Spectra were acquired in negative ion linear mode. The matrix used was a saturated solution of 6-aza-2-thiothymine in 50% acetonitrile and 10% tribasic ammonium citrate (9:1, v/v). Samples were dissolved in chloroform-methanol (4:1, v/v) and deposited on the sample plate, followed by an equal portion of matrix solution (0.5 µl).

Human Cell Isolation and Differentiation for Immune Stimulation Assays

Blood buffy coats were obtained from healthy volunteers after informed consent. The study protocol and any amendments were reviewed and approved by an independent review board (New England IRB, Newton, MA, USA) before the start of the study. The study was conducted according to the ethical principles of the Declaration of Helsinki.

PBMCs were freshly isolated from blood by Ficoll-Hypaque gradient centrifugation as previously described (Nair et al., 2012). Alternatively, where mentioned, PBMCs and cord blood mononuclear cells were purchased frozen from commercial suppliers. Monocyte-derived dendritic cells were differentiated *in vitro* from freshly isolated human monocytes as previously described (Nair et al., 2012). Briefly, CD14⁺ monocytes were isolated from freshly purified PBMCs by negative selection and magnetic bead sorting (Miltenyi). Cells were then incubated in complete RPMI 1640 in the presence of 50 ng/ml rhGM-CSF and 20 ng/ml rhIL-4 (R&D Systems) for 7 days.

***In vitro* LPS Stimulation Assays and Competition Assays**

PBMCs (10^5) or monocyte-derived dendritic cells (5×10^4) were incubated in the presence of LPS purified from various strains (Table S3) at doses ranging from 10^{-3} to 10^4 ng/ml for 18-20 h. For inhibition assays, cells were stimulated simultaneously with 100 pg/ml of LPS purified from *E. coli*. Supernatants were collected and analyzed using the cytokine bead array human inflammation kit (BD Biosciences) according to the manufacturer's instructions. Groups were compared using two-tailed non-homoscedastic t-test corrected for multiple testing by Sidak-Bonferroni using GraphPad Prism software.

Endotoxin Tolerance Assays

Endotoxin tolerance assays were adapted from the procedure described by Fresno et al. (del Fresno et al., 2009). Primary monocytes were isolated from human PBMCs and incubated in the presence of LPS purified from *B. dorei* or *E. coli* at doses ranging from 10^{-1} to 10^2 ng/ml for 18-20 h. Cells were then washed at least four times, and cultured in cRPMI. After 3 days of resting culture, monocytes were challenged with a standard dose of 5 µg/ml of zymosan. Supernatants were collected after 20 h and analyzed using the cytokine bead array human inflammation kit (BD Biosciences) according to the manufacturer's instructions.

HEK293 NFκB Reporter Cell Assays

HEK293 cells (5×10^4) stably expressing the NFκB-inducible Lucia luciferase reporter gene and human TLR4a, CD14, and MD2 genes (5×10^4) were seeded in 96-well plates and stimulated with doses of LPS purified from various strains (Table S3) at doses ranging from 10^{-3} to 10^4 ng/ml for 6-8 h. For inhibition assays, cells were stimulated simultaneously with 1 ng/ml of LPS purified from *E. coli*. Luciferase activity was measured by BrightGlo (Promega) according to the manufacturer's instructions. HEK293 reporter cells were purchased from InvivoGen. All cell lines were tested for mycoplasma contamination using PCR-based assay by an independent service provider.

Diabetes incidence in NOD mice

Mice were maintained in specific-pathogen-free facilities at Novartis Institutes for Biomedical Research (NIBR) facilities in Cambridge, MA. All animal studies were conducted under protocols approved by the Institutional Animal Care and Use Committee (IACUC) at NIBR. NOD/ShiLTj mice were purchased from Jackson Laboratory. Groups of 9 to 12, 8-week old mice were injected intraperitoneally with 10 µg LPS purified from either *E. coli* or *B. dorei* once a week for 4 consecutive weeks. Non-fasting blood glucose was monitored weekly. The experimenter was blinded to the nature of the treatment for each group. Animals with either one reading above 300 mg/dL or two consecutive readings above 250 mg/dL were deemed diabetic.

Full List of DIABIMMUNE Study Group Members

The members of the DIABIMMUNE Study Group are Mikael Knip, Katriina Koski, Matti Koski, Taina Härkönen, Samppa Ryhänen, Heli Siljander, Anu-Maria Hääläinen, Anne Ormisson, Aleksandr Peet, Vallo Tillmann, Valentina Ulrich, Elena Kuzmicheva, Sergei Mokurov, Svetlana Markova, Svetlana Pylova, Marina Isakova, Elena Shakurova, Vladimir Petrov, Natalya V. Dorshakova, Tatyana Karapetyan, Tatyana Varlamova, Jorma Ilonen, Minna Kiviniemi, Kristi Alnek, Helis Janson, Raivo Uibo, Tiit Salum, Erika von Mutius, Juliane Weber, Helena Ahlfors, Henna Kallionpää, Essi Laajala, Riitta Lahesmaa, Harri Lähdesmäki, Robert Molder, Viveka Öling, Janne Nieminen, Terhi Ruohutula, Outi Vaarala, Hanna Honkanen, Heikki Hyöty, Anita Kondrashova, Sami Oikarinen, Hermie J.M. Harmsen, Marcus C. De Goffau, Gjal Welling, Kirsi Alahuhta, Tuuli Korhonen, Suvi M. Virtanen, and Taina Öhman.

Supplemental References

- Abubucker, S., Segata, N., Goll, J., Schubert, A.M., Izard, J., Cantarel, B.L., Rodriguez-Mueller, B., Zucker, J., Thiagarajan, M., Henrissat, B., *et al.* (2012). Metabolic reconstruction for metagenomic data and its application to the human microbiome. *PLoS computational biology* *8*, e1002358.
- Atarashi, K., Tanoue, T., Shima, T., Imaoka, A., Kuwahara, T., Momose, Y., Cheng, G., Yamasaki, S., Saito, T., Ohba, Y., *et al.* (2011). Induction of colonic regulatory T cells by indigenous Clostridium species. *Science* *331*, 337-341.
- Buchfink, B., Xie, C., and Huson, D.H. (2015). Fast and sensitive protein alignment using DIAMOND. *Nat Methods* *12*, 59-60.
- del Fresno, C., Garcia-Rio, F., Gomez-Pina, V., Soares-Schanoski, A., Fernandez-Ruiz, I., Jurado, T., Kajiji, T., Shu, C., Marin, E., Gutierrez del Arroyo, A., *et al.* (2009). Potent phagocytic activity with impaired antigen presentation identifying lipopolysaccharide-tolerant human monocytes: demonstration in isolated monocytes from cystic fibrosis patients. *J Immunol* *182*, 6494-6507.
- Dimmer, E.C., Huntley, R.P., Alam-Faruque, Y., Sawford, T., O'Donovan, C., Martin, M.J., Bely, B., Browne, P., Mun Chan, W., Eberhardt, R., *et al.* (2012). The UniProt-GO Annotation database in 2011. *Nucleic Acids Res* *40*, D565-570.
- Faith, J.J., Guruge, J.L., Charbonneau, M., Subramanian, S., Seedorf, H., Goodman, A.L., Clemente, J.C., Knight, R., Heath, A.C., Leibl, R.L., *et al.* (2013). The long-term stability of the human gut microbiota. *Science* *341*, 1237439.
- Gene Ontology, C. (2015). Gene Ontology Consortium: going forward. *Nucleic Acids Res* *43*, D1049-1056.
- Gevers, D., Kugathasan, S., Denzon, L.A., Vazquez-Baeza, Y., Van Treuren, W., Ren, B., Schwager, E., Knights, D., Song, S.J., Yassour, M., *et al.* (2014). The treatment-naïve microbiome in new-onset Crohn's disease. *Cell Host Microbe* *15*, 382-392.
- Hirschfeld, M., Ma, Y., Weis, J.H., Vogel, S.N., and Weis, J.J. (2000). Cutting edge: repurification of lipopolysaccharide eliminates signaling through both human and murine toll-like receptor 2. *Journal of immunology* *165*, 618-622.
- Huang, K., Brady, A., Mahurkar, A., White, O., Gevers, D., Huttenhower, C., and Segata, N. (2014). MetaRef: a pan-genomic database for comparative and community microbial genomics. *Nucleic Acids Res* *42*, D617-624.
- Huang, Y., Li, H., Hu, H., Yan, X., Waterman, M.S., Huang, H., and Zhou, X.J. (2007). Systematic discovery of functional modules and context-specific functional annotation of human genome. *Bioinformatics* *23*, i222-229.
- Knights, D., Kuczynski, J., Charlson, E.S., Zaneveld, J., Mozer, M.C., Collman, R.G., Bushman, F.D., Knight, R., and Kelley, S.T. (2011a). Bayesian community-wide culture-independent microbial source tracking. *Nat Methods* *8*, 761-763.
- Knights, D., Kuczynski, J., Koren, O., Ley, R.E., Field, D., Knight, R., DeSantis, T.Z., and Kelley, S.T. (2011b). Supervised classification of microbiota mitigates mislabeling errors. *ISME J* *5*, 570-573.
- Kostic, A.D., Gevers, D., Siljander, H., Vatanen, T., Hyotylainen, T., Hamalainen, A.M., Peet, A., Tillmann, V., Poho, P., Mattila, I., *et al.* (2015). The dynamics of the human infant gut microbiome in development and in progression toward type 1 diabetes. *Cell host & microbe* *17*, 260-273.
- Langmead, B., and Salzberg, S.L. (2012). Fast gapped-read alignment with Bowtie 2. *Nat Methods* *9*, 357-359.
- Lee, D.H., Bae, J.E., Lee, J.H., Shin, J.S., and Kim, I.S. (2010). Quantitative detection of residual *E. coli* host cell DNA by real-time PCR. *J Microbiol Biotechnol* *20*, 1463-1470.

- Luo, C., Knight, R., Siljander, H., Knip, M., Xavier, R.J., and Gevers, D. (2015). ConStrains identifies microbial strains in metagenomic datasets. *Nature biotechnology* 33, 1045-1052.
- McDonald, D., Price, M.N., Goodrich, J., Nawrocki, E.P., DeSantis, T.Z., Probst, A., Andersen, G.L., Knight, R., and Hugenholtz, P. (2012). An improved Greengenes taxonomy with explicit ranks for ecological and evolutionary analyses of bacteria and archaea. *ISME J* 6, 610-618.
- Morgan, X.C., Tickle, T.L., Sokol, H., Gevers, D., Devaney, K.L., Ward, D.V., Reyes, J.A., Shah, S.A., LeLeiko, N., Snapper, S.B., *et al.* (2012). Dysfunction of the intestinal microbiome in inflammatory bowel disease and treatment. *Genome biology* 13, R79.
- Nair, S., Archer, G.E., and Tedder, T.F. (2012). Isolation and generation of human dendritic cells. *Curr Protoc Immunol Chapter 7*, Unit7 32.
- Nakatsuji, T., Chiang, H.I., Jiang, S.B., Nagarajan, H., Zengler, K., and Gallo, R.L. (2013). The microbiome extends to subepidermal compartments of normal skin. *Nat Commun* 4, 1431.
- Odamaki, T., Xiao, J.Z., Sakamoto, M., Kondo, S., Yaeshima, T., Iwatsuki, K., Togashi, H., Enomoto, T., and Benno, Y. (2008). Distribution of different species of the *Bacteroides fragilis* group in individuals with Japanese cedar pollinosis. *Appl Environ Microbiol* 74, 6814-6817.
- Sela, D.A., Chapman, J., Adeuya, A., Kim, J.H., Chen, F., Whitehead, T.R., Lapidus, A., Rokhsar, D.S., Lebrilla, C.B., German, J.B., *et al.* (2008). The genome sequence of *Bifidobacterium longum* subsp. *infantis* reveals adaptations for milk utilization within the infant microbiome. *Proceedings of the National Academy of Sciences of the United States of America* 105, 18964-18969.
- Suzek, B.E., Wang, Y., Huang, H., McGarvey, P.B., Wu, C.H., and UniProt, C. (2015). UniRef clusters: a comprehensive and scalable alternative for improving sequence similarity searches. *Bioinformatics* 31, 926-932.
- Tickle, T.L., Segata, N., Waldron, L., Weingart, U., and Huttenhower, C. (2013). Two-stage microbial community experimental design. *ISME J* 7, 2330-2339.
- Truong, D.T., Franzosa, E.A., Tickle, T.L., Scholz, M., Weingart, G., Pasolli, E., Tett, A., Huttenhower, C., and Segata, N. (2015). MetaPhlAn2 for enhanced metagenomic taxonomic profiling. *Nature methods* 12, 902-903.
- UniProt, C. (2015). UniProt: a hub for protein information. *Nucleic Acids Res* 43, D204-212.
- Zhou, X., Kao, M.C., and Wong, W.H. (2002). Transitive functional annotation by shortest-path analysis of gene expression data. *Proc Natl Acad Sci U S A* 99, 12783-12788.
- Zhou, Z., Lin, S., Cotter, R.J., and Raetz, C.R. (1999). Lipid A modifications characteristic of *Salmonella typhimurium* are induced by NH4VO3 in *Escherichia coli* K12. Detection of 4-amino-4-deoxy-L-arabinose, phosphoethanolamine and palmitate. *J Biol Chem* 274, 18503-18514.
- Zhou, Z., White, K.A., Polissi, A., Georgopoulos, C., and Raetz, C.R. (1998). Function of *Escherichia coli* MsbA, an essential ABC family transporter, in lipid A and phospholipid biosynthesis. *J Biol Chem* 273, 12466-12475.

Table S3. Bacterial Strains used in LPS Purification, Related to Figure 4

Name	Description	Reference
<i>Bacteroides dorei</i>	strain: 175	DSM 17855
<i>Bacteroides ovatus</i>	strain: NCTC11153	ATCC 8483
<i>Bacteroides vulgatus</i>	strain: NCTC11154	ATCC 8482
<i>Bacteroides stercoris</i>	strain: VPIB5-21	ATCC 43183
<i>Bacteroides fragilis</i>	strain: VPI2553	ATCC 25285
<i>Bacteroides uniformis</i>	strain: VPI0061	ATCC 8492
<i>Bacteroides caccae</i>	strain: VPI3452A	ATCC 43185
<i>Prevotella copri</i>	strain: 18205	DSM 18205
<i>Akkermansia mucinophila</i>	strain: CIP107961	ATCC BAA-835
<i>Klebsiella oxytoca</i>	strain: OCC-SAL-18A	ATCC 68831
<i>Escherichia coli</i>	strain: ECOR2	Ochman & Selander, J. Bacteriol (1984)

Table S3. Bacterial Strains used in LPS Purification, Related to Figure 4

A list of bacterial strains that were used in the LPS purification experiments.